



HAL
open science

A family of protein-deglutamylating enzymes associated with neurodegeneration.

Krzysztof Rogowski, Juliette van Dijk, Maria M. Magiera, Christophe Bosc, Jean-Christophe Deloulme, Anouk Bosson, Leticia Peris, Nicholas D. Gold, Benjamin Lacroix, Montserrat Bosch Grau, et al.

► To cite this version:

Krzysztof Rogowski, Juliette van Dijk, Maria M. Magiera, Christophe Bosc, Jean-Christophe Deloulme, et al.. A family of protein-deglutamylating enzymes associated with neurodegeneration.. *Cell*, 2010, 143 (4), pp.564-78. 10.1016/j.cell.2010.10.014 . hal-00538184

HAL Id: hal-00538184

<https://hal.science/hal-00538184>

Submitted on 25 Nov 2010

HAL is a multi-disciplinary open access archive for the deposit and dissemination of scientific research documents, whether they are published or not. The documents may come from teaching and research institutions in France or abroad, or from public or private research centers.

L'archive ouverte pluridisciplinaire **HAL**, est destinée au dépôt et à la diffusion de documents scientifiques de niveau recherche, publiés ou non, émanant des établissements d'enseignement et de recherche français ou étrangers, des laboratoires publics ou privés.

A family of protein deglutamylating enzymes associated with neurodegeneration

Krzysztof Rogowski^{1#}, Juliette van Dijk¹, Maria M. Magiera^{1,2,3,4}, Christophe Bosc⁵, Jean-Christophe Deloulme⁵, Anouk Bosson⁵, Leticia Peris⁵, Nicholas D. Gold¹, Benjamin Lacroix¹, Montserrat Bosch Grau^{1,2,3,4}, Nicole Bec⁶, Christian Larroque⁶, Solange Desagher⁷, Max Holzer⁸, Annie Andrieux⁵, Marie-Jo Moutin⁵ and Carsten Janke^{1,2,3,4#}

¹CRBM, Université Montpellier 2 and 1, CNRS, 34293 Montpellier, France;

²present address: Institut Curie, 91405 Orsay, France;

³present address: CNRS UMR 3306, 91405 Orsay, France;

⁴present address: INSERM U1005, 91405 Orsay, France;

⁵INSERM U836, Grenoble Institut des Neurosciences, CEA-iRTSV-GPC, Université Joseph Fourier, BP170, 38042 Grenoble, France;

⁶CRLC Val d'Aurelle, Institut de Recherche en Cancérologie de Montpellier, INSERM, 34298 Montpellier, France;

⁷IGMM, Université Montpellier 2, CNRS, 34293 Montpellier, France;

⁸Paul-Flechsig-Institute of Brain Research, University of Leipzig, 04109 Leipzig, Germany

#corresponding authors:

Krzysztof Rogowski, CRBM, CNRS, 1919 route de Mende, 34293 Montpellier, France

Telephone: +33 4 67613335

Fax: +33 4 67521559

Email: krzysztof.rogowski@crbm.cnrs.fr

Carsten Janke, Institut Curie, Bat 110 - Centre Universitaire, 91405 Orsay, France

Telephone: +33 1 69863127

Fax: +33 1 69863017

Email: Carsten.Janke@curie.fr

Keywords: Tubulin, microtubules, polyglutamylation, deglutamylation, cytosolic carboxy peptidase, CCP, *pcd* mouse, neurodegeneration, Nna1, polyglutamylase, TTLL

SUMMARY

Polyglutamylation is a posttranslational modification that generates glutamate side chains on tubulins and other proteins. Although this modification has been shown to be reversible, little is known about the enzymes catalyzing deglutamylation. Here we describe the enzymatic mechanism of protein deglutamylation by members of the cytosolic carboxypeptidase (CCP) family. Three enzymes (CCP1, CCP4 and CCP6) catalyze the shortening of polyglutamate chains while a fourth (CCP5) specifically removes the branching point glutamates. In addition, CCP1, CCP4 and CCP6 also remove gene-encoded glutamates from the carboxy-termini of proteins. Accordingly, we show that these enzymes convert detyrosinated tubulin into $\Delta 2$ -tubulin, and also modify other substrates, including myosin light chain kinase 1. We further analyze *purkinje cell degeneration (pcd)* mice that lack functional CCP1 and show that microtubule hyperglutamylation is directly linked to neurodegeneration. Taken together, our results reveal that controlling the length of the polyglutamate side chains on tubulin is critical for neuron survival.

HIGHLIGHTS

- Posttranslational polyglutamylation is reversed by cytosolic carboxypeptidases
- Removal of C-terminal glutamates is a novel posttranslational modification
- Neuronal degeneration is directly linked to tubulin hyperglutamylation

INTRODUCTION

Polyglutamylation is a posttranslational modification that generates glutamate side chains of variable length on the γ -carboxyl groups of glutamic acid residues within the primary sequence of the target proteins. This modification has been initially discovered on α - and β -tubulin, the building blocks of microtubules (MTs; Eddé et al., 1990; Rüdiger et al., 1992), and later also found on other proteins (Regnard et al., 2000; van Dijk et al., 2008).

Polyglutamylation levels are particularly high on stable MT assemblies such as the ones found in neurons (Audebert et al., 1993), axonemes (Bré et al., 1994), centrioles and basal bodies (Bobinnec et al., 1998), but is also enriched in the highly dynamic mitotic spindle (Regnard et al., 1999). Tubulins are polyglutamylated at their carboxy-terminal tails, which upon assembly of MTs become exposed on the outer surface of the tubules, where they provide binding sites for several MT-associated proteins (MAPs) and molecular motors. Accordingly, MT polyglutamylation has recently been shown to regulate the activity of ciliary dynein (Kubo et al., 2010; Suryavanshi et al., 2010) and of the MT-severing protein spastin (Lacroix et al., 2010).

The enzymes that catalyze polyglutamylation, polyglutamylases, are members of a protein family sharing a homology domain with another tubulin modifying enzyme, tubulin tyrosine ligase (TTL; Ersfeld et al., 1993), and thus are referred to as TTL-like (TTLL) proteins (Janke et al., 2005; van Dijk et al., 2007). Initial functional studies on polyglutamylases provided first evidence that polyglutamylation plays important roles *in vivo*. Mice knocked out for TTLL1 polyglutamylase display abnormal beating of airway epithelial cilia leading to respiratory problems (Ikegami et al., 2010). Another polyglutamylase, TTLL6, was also shown to play a role in cilia. Depletion of this enzyme in zebrafish reduced glutamylation in the olfactory placodes resulting in defective assembly of olfactory cilia (Pathak et al., 2007). Surprisingly, also overexpression of TTLL6 enzyme, which caused abnormal elongation of

glutamate chains, produced ciliary defects in *Tetrahymena* (Janke et al., 2005; Wloga et al., 2009). Taken together, this suggests that maintaining the correct levels of tubulin polyglutamylation by the coordinated action of polyglutamylases and deglutamylating enzymes is essential. The aim of the present work was to identify deglutamylating enzymes and analyze their functions in vivo.

Recent studies of a family of cytosolic carboxypeptidases (CCP) have suggested that one of the members of this family, CCP1 (also known as Nna1), is the enzyme that removes the C-terminal tyrosine from α -tubulin (Kalinina et al., 2007; Rodriguez de la Vega et al., 2007), however convincing evidence has not been provided. The possibility that CCP1 is involved in tubulin modifications was exciting since loss of function of CCP1 had been associated with the phenotypes observed in Purkinje Cell Degeneration (*pcd*) mice (Fernandez-Gonzalez et al., 2002). *Pcd* mice display multiple defects including degeneration of several types of neurons. The first neurons to be lost are Purkinje cells, which die during early adulthood leading to ataxia. The loss of Purkinje cells is followed by degeneration of cerebellar granule neurons (CGNs) and later some populations of thalamic neurons also disappear (Mullen et al., 1976). Moreover, mitral cells from the olfactory bulb as well as retinal photoreceptors degenerate progressively over one year. Finally, the males are sterile and the females experience difficulties giving birth (reviewed in: Wang and Morgan, 2007). Recent studies demonstrated that Purkinje cell loss as well as retinal degeneration observed in the *pcd* mice could be rescued by wild type (WT) CCP1, but not an inactive CCP1 (Chakrabarti et al., 2008; Wang et al., 2006). This demonstrated that the lack of CCP1 carboxypeptidase activity is responsible for the phenotypes observed in the *pcd* mice, however, the molecular mechanisms underlying the numerous defects remain unclear.

Here, we show that CCP1 specifically catalyzes the removal of the penultimate glutamate residue from detyrosinated α -tubulin thus generating $\Delta 2$ -tubulin, however it is not involved in

detyrosination itself. Moreover, we demonstrate that the removal of gene-encoded glutamic acids from the C-termini of proteins is not specific to tubulin, but affects a range of substrates including myosin light chain kinase 1 (MLCK1). Apart from the deglutamylation of protein primary sequence, CCP1 also shortens posttranslationally generated glutamate side chains on tubulin, and is therefore a tubulin deglutamylase. We further demonstrate the existence of two functional homologs of CCP1, CCP4 and CCP6, and we provide evidence that another recently described deglutamylating enzyme, CCP5 (Kimura et al., 2010), specifically removes the branching point glutamates generated by polyglutamylation. Finally, we have analyzed the neurodegeneration phenotype in the *pcd* mice in the light of the newly identified deglutamylating activity of CCP1. Consistently with the enzymatic activity of CCP1, we show that tubulin polyglutamylation is highly increased specifically in brain areas that degenerate in the *pcd* mice. Moreover, by downregulating polyglutamylation, we were able to partially prevent neurodegeneration providing direct evidence that abnormally high polyglutamylation levels lead to neuronal degeneration.

RESULTS

CCP1 generates $\Delta 2$ -tubulin and also acts as tubulin deglutamylase

Recent studies have suggested that CCP1 is involved in α -tubulin detyrosination (Kalinina et al., 2007). To directly test this idea, we performed immunoblot analysis of protein extracts prepared from HEK293 cells expressing either active or enzymatically inactive (dead, Fig. S1) murine CCP1. While we did not observe any increase in the level of tubulin detyrosination, we detected an ectopic appearance of a related tubulin modification, $\Delta 2$ -tubulin (Paturle-Lafanechere et al., 1991). Thus, CCP1 seems to catalyze the removal of the penultimate glutamate residue, but not detyrosination itself. To further test if CCP1 is specifically generating $\Delta 2$ -tubulin, we expressed this protein in mouse embryonic fibroblasts (MEFs) and stained the cells with antibodies for tyrosinated and $\Delta 2$ -tubulin. There was no obvious reduction in the level of tyrosinated tubulin, but we observed a strong increase in the labeling for $\Delta 2$ -tubulin specifically in cells expressing CCP1 (Fig. 1B). This increase in the level of $\Delta 2$ -tubulin was not observed when the enzymatically dead version of CCP1 was expressed (Fig. S2A). Taken together these results demonstrate that CCP1 catalyzes the removal of the very C-terminal glutamate residue from detyrosinated α -tubulin, but it is not involved in α -tubulin detyrosination.

Considering that CCP1 was associated with α -tubulin primary sequence deglutamylation, we speculated that it might also catalyze the removal of glutamate side chains, which are added to α - and β -tubulin as a result of posttranslational polyglutamylation (Eddé et al., 1990; Rüdiger et al., 1992). To test this hypothesis, we expressed CCP1 in neurons, which are known to carry a high level of tubulin polyglutamylation (Audebert et al., 1993), and labeled them with polyE antibody that recognizes glutamate chains composed of at least three glutamic acids (Fig. S4C). Neurons expressing active but not inactive CCP1 showed a strong

reduction in the level of polyE signal (Fig. 1C; S2B). These results show that CCP1 is indeed involved in the removal of posttranslational polyglutamylation.

To further characterize the deglutamylation activity of CCP1 we set up an *in vitro* deglutamylation assay in which highly polyglutamylated brain tubulin was incubated with protein extract from HEK293 cells expressing either active or inactive CCP1. The status of polyglutamylation was examined with two polyglutamylation specific antibodies: polyE that recognizes long glutamate side chains, and GT335 that recognizes all glutamylated forms of tubulin because it is specific to the branching point of the glutamate side chain (Wolff et al., 1992). In combination, these two antibodies allowed us to distinguish between tubulin carrying either short or long glutamate side chains. Brain tubulin treated with active CCP1 was no longer detected by polyE antibodies, while the GT335 signal was not decreased (Fig. 1D). This indicated that CCP1 shortens the glutamate side chains of brain tubulin without removing the branching point glutamates. Similar results were obtained with purified 6His-CCP1, confirming that CCP1 directly catalyzes tubulin deglutamylation (Fig. S2C, D). To further investigate the enzymatic specificity of CCP1 for long side chains, we assayed the enzyme with mono- or polyglutamylated tubulin purified from HeLa cells after overexpression of different TLL glutamylating enzymes (Lacroix et al., 2010; van Dijk et al., 2007). When monoglutamylated tubulin (modified by TLL4) was incubated with active CCP1, no changes in glutamylation levels were observed, indicating that CCP1 cannot remove the short side chains generated by TLL4 (Fig. 1D). Surprisingly, when tubulin polyglutamylated with TLL6 was incubated with CCP1, a strong reduction in both polyE and GT335 signals was observed (Fig. 1D). This indicated that besides shortening the polyglutamate side chains, CCP1 also removes the branching point glutamates when the glutamylation is generated by TLL6 but not by TLL4 or by TLL1, which generates most of the glutamylation present on brain MTs (Janke et al., 2005). To validate that the removal of

the branching point glutamates by CCP1 depends on the enzyme that has generated glutamylation in the first place, we set up co-transfection experiments. CCP1 was co-expressed together with TLL4 or TLL6 in HEK293 cells, and the cell extracts were analyzed by immunoblot. In agreement with our *in vitro* data, expression of CCP1 had no effect on the glutamylation status of tubulin and other proteins that are modified by TLL4. In contrast, CCP1 blocked the accumulation of both, mono- and polyglutamylation on TLL6 substrates, which include tubulins and TLL6 itself (Fig. 1E). These results confirmed that CCP1, in addition to shortening of long glutamate chains, also removes the branching point glutamates when the modification is generated by TLL6 but not TLL4.

Tubulin modifications in the *pcd* mouse that lacks active CCP1

To study the role of CCP1 *in vivo* we took advantage of Purkinje Cell Degeneration (*pcd*^{*3J*}) mice in which a deletion in the *CCP1* gene results in loss of function of the CCP1 protein (Fernandez-Gonzalez et al., 2002). Based on our discovery of the deglutamylating activity of CCP1 we expected the absence of $\Delta 2$ -tubulin and increased tubulin polyglutamylation in the *pcd* mice. To test our predictions we compared the status of tubulin modifications between *pcd* and WT mice. Protein extracts from several organs were analyzed by immunoblot with antibodies recognizing either the unmodified C-terminal α -tubulin tail (tyrosinated tubulin) or its processed versions (detyrosinated or $\Delta 2$ -tubulin), as well as with polyE antibodies specific to long glutamate chains. When comparing the levels of tyrosinated and detyrosinated tubulin between *pcd* and WT mice we observed no differences in all organs analyzed. Surprisingly, the $\Delta 2$ -tubulin modification was also unchanged in most of the organs except skeletal muscles, where we detected a strong reduction (Fig. 2A). This confirmed that CCP1 is involved in generating $\Delta 2$ -tubulin *in vivo*, but at the same time it implied the existence of additional enzyme(s) catalyzing this modification. Tubulin polyglutamylation, for which we expected an increase in the *pcd* mice, at least in the organs where tubulin glutamylases are

highly expressed such as brain and testes, was indeed slightly increased relative to the equal levels of tyrosinated tubulin in these two organs (Fig. 2A). These results are in agreement with CCP1 being involved in the removal of posttranslational tubulin polyglutamylation.

In contrast to mostly slight changes in the levels of tubulin posttranslational modifications observed in the *pcd* mice, we detected protein bands outside of the tubulin region that reacted with anti- $\Delta 2$ -tubulin exclusively in the WT mice. Conversely, bands of corresponding size were labeled by detyrosinated or polyE antibodies in the *pcd* mice (Fig. 2A). This suggested the existence of proteins that end with a $-GE_n$ sequence at their C-termini, which is recognized in the *pcd* mice with polyE (if $n \geq 3$) or with detyrosinated antibody (if $n=2$). However, in WT mice, both types of proteins have C-termini shortened to $-GE$ (specifically detected with anti- $\Delta 2$ -tubulin antibody), most likely by the enzymatic activity of CCP1. Thus, C-terminal deglutamylation seems to be a modification that is not restricted to tubulin.

MLCK1 and telokin are substrates of CCP1

Two of the potential CCP1 substrates (~ 130 kDa and ~ 20 kDa) were prominent in stomach and one (~ 130 kDa) in the uterus (Fig. 2A). In order to identify these substrates, we prepared protein extract from mouse stomach and analyzed the two anti- $\Delta 2$ -reactive bands by mass spectrometry. Several proteins were identified (Table S2, S3), but only two appeared as promising candidates for being processed by CCP1. Myosin Light Chain kinase 1 (130 kDa-MLCK1) and telokin, a 17-kDa protein corresponding to the C-terminal fragment of MLCK1 (Smith et al., 1998), end with the sequence $-EGEEGGEEEEEEEE$. Thus, both proteins could be detected with polyE, or when processed by CCP1 to $-EGEEGGGE$ with anti- $\Delta 2$ -tubulin antibody. To provide additional evidence that MLCK1 undergoes C-terminal deglutamylation, we used an anti-MLCK antibody for immunoprecipitation from stomach and uterus extracts and showed that the immunoprecipitated protein was detected by anti- $\Delta 2$ -tubulin antibodies (Fig. 2B). To demonstrate that MLCK and telokin are processed by CCP1,

we expressed them together with active or inactive CCP1 in HEK293 cells and analyzed the protein extracts by immunoblot (see Fig. S4C for antibody specificities). In the presence of inactive CCP1, both MLCK1 and telokin were recognized by polyE but not anti- $\Delta 2$ -tubulin antibodies. In contrast, when MLCK1 and telokin were expressed together with active CCP1, both proteins were labeled by anti- $\Delta 2$ -tubulin but not polyE antibodies (Fig. 2C). To confirm that CCP1 directly catalyzes primary sequence deglutamylation, we incubated purified GST-telokin with purified 6His-CCP1. GST-telokin treated with CCP1 was recognized by anti- $\Delta 2$ -tubulin but not polyE antibodies demonstrating that CCP1 shortened the C-terminal glutamate stretch (Fig. 2D). Primary sequence deglutamylation was no longer observed in the presence of phenanthroline, a specific inhibitor of metalloproteases (Fig. 2D). These results clearly show that MLCK1 and telokin are directly processed by CCP1 in the way that seven out of eight C-terminal glutamates are removed from the C-termini of these proteins.

Finally, we tested if CCP1 activity is restricted to the removal of glutamates, or if this enzyme could potentially also process other amino acids. Based on telokin, we generated several artificial substrates ending with the C-terminal sequences -GED, -GEEDD, -GEEY and -GEEF. All of these artificial telokins including WT telokin were co-transfected with CCP1 in HEK293 cells and the protein extracts were analyzed with anti- $\Delta 2$ -tubulin antibodies on immunoblot. Only WT telokin was detected with anti- $\Delta 2$ -tubulin antibody (Fig. 2E), indicating that CCP1 is a highly specific carboxypeptidase that exclusively cuts peptide bonds between two C-terminally located glutamates. Even aspartate, the amino acid that most closely resembles glutamate, was not removed by CCP1. In addition, aromatic residues such as tyrosine and phenylalanine were also blocking deglutamylation of telokin, which is coherent with our data indicating that CCP1 does not catalyze α -tubulin detyrosination.

CCP4 and CCP6 also generate $\Delta 2$ -tubulin and act as long-chain deglutamylases

Our observation that in most of the organs of the *pcd* mice, except skeletal muscles, $\Delta 2$ -tubulin levels are comparable to WT mice (Fig. 2A) clearly showed that additional enzyme(s) are involved in $\Delta 2$ -tubulin generation. The CCP protein family, apart from CCP1, contains five additional members (Kalinina et al., 2007; Rodriguez de la Vega et al., 2007). We tested if any of the other CCPs generates $\Delta 2$ -tubulin by expressing them in MEFs. Immunofluorescence analysis with anti-tyrosinated and anti- $\Delta 2$ -tubulin antibodies demonstrated that in addition to CCP1, also CCP4 and CCP6 generate $\Delta 2$ -tubulin (Fig. 3A, S3A). This result was confirmed by immunoblot analysis of HEK293 cells transfected with CCP4 and CCP6 (Fig. S3B, C). The level of tyrosinated tubulin in cells expressing CCP4 and CCP6 remained unchanged, indicating that these enzymes, similarly to CCP1, do not detyrosinate tubulin (Fig. 3A). We further tested whether CCP4 and CCP6 also remove polyglutamylation. Using *in vitro* deglutamylation assays with brain tubulin and protein extracts from HEK293 cells expressing either CCP4 or CCP6, we observed a strong reduction in the polyE but not GT335 signal (Fig. 3B, C). Finally, we tested if CCP4 and CCP6 also remove glutamates from the primary sequence of MLCK1 and telokin. After co-expressing MLCK or telokin with CCP4 or CCP6 in HEK293 cells, both substrates were labeled with anti- $\Delta 2$ -tubulin, but not polyE antibodies (Fig. S4A, B). Thus CCP4 and CCP6 generate $\Delta 2$ -tubulin, catalyze shortening of glutamate side chains and remove all but one of the C-terminal glutamates from MLCK1 and telokin, indicating that they are functional homologs of CCP1.

Progressive accumulation of polyglutamylation in the cerebellum and olfactory bulb of the *pcd* mice

Our immunoblot analysis of tubulin posttranslational modifications demonstrated that tubulin polyglutamylation is slightly increased in the brain of adult *pcd* mice (Fig. 2A). To test if this increase was confined to regions where neurodegeneration occurred, we analyzed the status of tubulin modifications in cerebellum, a part of the brain with extensive

degeneration, and in cerebral cortex where no degeneration has been observed. Protein extracts from P7, P14, P21, or adult WT and *pcd* mice were analyzed by immunoblot using antibodies specific to tubulin modifications. At early developmental stages, $\Delta 2$ -tubulin levels were strongly reduced in both cerebellum and cortex of the *pcd* mice as compared to WT (Fig. 4A, B; lanes “P7”; Fig. S5A). At later stages, $\Delta 2$ -tubulin gradually increased reaching WT levels in adult mice. However, the restoration of $\Delta 2$ -tubulin modification occurred earlier in the cortex as compared to the cerebellum (Fig. 4A, B).

Consistent with the deglutamylation activity of CCP1, the degree of tubulin polyglutamylation was strongly increased in cortex and cerebellum of young *pcd* mice (Fig. 4A, B; lanes “P7”; Fig. S5A). At later stages of development, polyglutamylation in the cortex was progressively reduced to WT levels, while it continued to increase in the cerebellum of the *pcd* mice. Moreover, the tubulin from the cerebellum of adult *pcd* mice migrated slightly slower on the protein gel, which emphasizes the strong accumulation of long polyglutamate chains on tubulin (Fig. 4A, B; lanes “adult”). An unrelated tubulin modification, acetylation, was not significantly affected in *pcd* mice at all developmental stages (Fig. 4A, B). This shows that not all tubulin modifications are changed in the *pcd* mice, and that the changes observed for $\Delta 2$ -tubulin and polyglutamylation are likely to be a direct result of the lack of CCP1 deglutamylating activity.

It was striking that polyglutamylation, which is strongly increased in both cerebellum and cortex of the *pcd* mice at earlier developmental stages, returns to WT levels in adult mice only in the cortex, but not in cerebellum (Fig. 4A, B). This implies the existence of a compensation mechanism that would operate in cortex, but would be inefficient in the cerebellum. A compensating mechanism for CCP1 is likely to involve enzymes with similar reaction specificities, such as CCP4 and CCP6. *In situ* hybridization studies have previously shown that CCP1 is highly expressed in cerebellum and cortex of adult mouse brain, whereas CCP6

expression was rather restricted to cortex, and CCP4 appeared to be generally expressed at low levels (Kalinina et al., 2007). We compared the expression levels of CCP1, CCP4 and CCP6 in cortex and cerebellum at different developmental stages by reverse transcription polymerase chain reaction (Fig. S5B). While CCP1 appeared to be expressed at similar levels in both cerebellum and cortex throughout all developmental stages, CCP6 expression was very low in cerebellum as compared to cortex. CCP4 expression was generally much lower in comparison to CCP1 and CCP6 (visible only after 35 PCR cycles versus 25 cycles for CCP1 and CCP6; Fig. S5B). Thus, it is possible that CCP6 compensates for the absence of CCP1 in the cortex of the *pcd* mice, whereas it is present at too low levels to achieve a complete compensation in cerebellum. As a consequence, unopposed polyglutamylase activity results in tubulin hyperglutamylation in cerebellum. Strikingly, $\Delta 2$ -tubulin generation, which is also catalyzed by CCP1, is compensated in the cerebellum of the *pcd* mice, although less efficiently than in cortex (Fig. 4A, B). This might be best explained by the fact that $\Delta 2$ -tubulin generation is irreversible (Paturle-Lafanechere et al., 1991), thus allowing for progressive accumulation of this modification.

To test if the observed changes in tubulin modifications are directly related to neurons, we analyzed different types of neuronal cell cultures prepared from *pcd* and WT mice by immunoblot. Cerebellar granule neurons (CGNs) isolated from *pcd* mice at P7 and cultured for 7 days showed increased levels of polyglutamylation and decreased $\Delta 2$ -tubulin as compared to CGNs isolated from WT mice, whereas tubulin acetylation was unchanged. Similar results were obtained for primary cultures of cortical neurons isolated from WT and *pcd* mice at E17 and cultured for 7 days (Fig. 4C, D). Since both neuronal cultures contained only very low amounts of glia cells, these findings strongly suggest that the changes in tubulin modifications observed in the extracts of cerebellum and cortex of *pcd* mice are related to neurons.

The correlation between tubulin hyperglutamylation and neurodegeneration in the cerebellum of adult *pcd* mice suggested that degeneration of other regions of the brain in these mice might also be related to increased tubulin polyglutamylation. To test this hypothesis, we analyzed the status of tubulin modifications in the olfactory bulbs, known to undergo neurodegeneration in adult *pcd* mice. Similarly to cerebellum, we observed strong increase in the levels of tubulin polyglutamylation, while acetylation and $\Delta 2$ -tubulin levels were unchanged (Fig. 4E, F). Thus, our results suggested that neurodegeneration observed in the *pcd* mice is related to hyperglutamylation.

Purkinje cell degeneration in *pcd* mice is caused by hyperglutamylation

To unambiguously demonstrate the causal link between hyperglutamylation of tubulin observed in the *pcd* mice and neurodegeneration, we aimed to rescue the Purkinje cell degeneration by reducing the polyglutamylation levels in these neurons. Based on the observation that most of the tubulin polyglutamylase activity in brain is associated with the TTLL1-polyglutamylase complex (Janke et al., 2005), we used shRNA that specifically depletes TTLL1 to reduce polyglutamylation levels (Fig. S6). Lentivirus expressing TTLL1-specific shRNA (shTTLL1) and GFP, or control virus expressing only GFP were injected in the cerebellum of 10-d-old (P10) WT or *pcd* mice. The mice were analyzed 30 d after injection (P40) by behavioral tests and immunohistochemistry.

Analysis of cerebella from WT mice injected with control virus (n=6) showed that the differentiation of the Purkinje cell layer was not affected by the virus injections, and that some of the fully developed Purkinje cells expressed GFP, indicating that these cells were infected by the virus (Fig. 5A, B, panels WT + control virus). Cerebella from *pcd* mice injected with control virus (n=5) showed a complete degeneration of the Purkinje cell layer 30 d post-injection, which is in accordance with the expected degeneration of *pcd* mice cerebella at this age (Fig. 5A, panels *pcd* + control virus). In contrast, *pcd* mice cerebella

injected with shTTLL1 virus (n=6) displayed a large number of morphologically normal Purkinje cells in the injected (GFP-positive) regions of the brain, which was not the case in non-injected areas (Fig. 5A, B, panels *pcd* + virus shTTLL1). The rescue of Purkinje cell degeneration by the downregulation of TTLL1 polyglutamylase demonstrates that unopposed posttranslational polyglutamylation is the primary cause of the neuronal degeneration in the *pcd* mice.

To determine if mice injected with shTTLL1 virus have improved their motor coordination, we performed rotarod tests. Under our experimental conditions, *pcd* mice injected with control virus fell off the rod after ~12 s while *pcd* mice injected with shTTLL1 virus remained on the rod for ~22 s (Fig. 5C). Thus, injection of shTTLL1 virus in the cerebellum of *pcd* mice led to a significant improvement of the motor coordination of these mice.

CCP5 is a protein deglutamylase that specifically removes the branching point glutamates

Based on the analysis of CCP1, CCP4 and CCP6 it became obvious that none of these enzymes catalyzed the removal of branching point glutamates generated by TTLL4, or the ones present on mouse brain MTs. To identify the enzyme(s) responsible for the removal of these branching points, we screened the remaining CCP family members for such activity by co-expressing them with TTLL4. Using immunofluorescence, we identified CCP5 as the only enzyme that was able to remove TTLL4-dependent monoglutamylation in U2OS cells. This process was activity-dependent, as an inactive version of CCP5 did not prevent TTLL4-mediated glutamylation of MTs (Fig. 6A). To further characterize the specificity of CCP5, we compared the glutamylation levels in HEK293 cells co-expressing CCP5 with either TTLL4 or TTLL6 by immunoblots using GT335 and polyE antibodies. While co-expression of TTLL4 with inactive CCP5 induced monoglutamylation on several proteins, including α - and

β -tubulin, the co-expression with active CCP5 completely blocked the modification of the TLL4 substrates (Fig. 6B). This suggested that CCP5 removes glutamylation not only from tubulin but also from other substrates that were monoglutamylated by TLL4. In case of TLL6, expression with inactive CCP5 resulted in generation of GT335 and polyE signals on tubulins and TLL6 itself, while expression with active CCP5 completely removed monoglutamylation and strongly reduced polyglutamylation of tubulin. In addition, active CCP5 induced a slight reduction of the GT335 labeling of TLL6 protein band while the polyE signal remained unchanged, indicating that only short side chains are removed (Fig. 6B). Taken together these results clearly show that CCP5 removes branching point glutamates regardless if they were generated by TLL4 or TLL6.

To determine whether the reduction in polyE signal after co-expressing TLL6 with CCP5 is related to a long chain deglutamylase activity of CCP5, or if it was indirectly caused by the removal of short side chains prior to elongation, we tested CCP5 in an *in vitro* deglutamylation assay with brain tubulin. Brain MTs are known to carry mostly long glutamate chains on α -tubulin, whereas side chains on β -tubulin are predominantly short (Redeker et al., 2004). When brain tubulin was incubated with active CCP5, we observed complete removal of GT335 signal from β -tubulin, but only a slight reduction of the signal on α -tubulin. In contrast, no changes in the polyE signal were observed (Fig. 6C). These results strongly suggest that CCP5 activity is restricted to the removal of branching point glutamates, and that the enzyme does not shorten or remove long glutamate chains. To confirm this hypothesis, we performed additional *in vitro* assays using tubulin purified from HeLa cells overexpressing TLL4 (tubulin with short glutamate chains) or TLL6 (tubulin with long glutamate chains). While CCP5 completely removed GT335 signal from TLL4-modified tubulin, it only slightly reduced the GT335 labeling on TLL6-modified tubulin, and did not affect the polyE labeling. Together with the observation that CCP5 does not generate $\Delta 2$ -

tubulin (not shown), these data are in agreement with CCP5 being a deglutamylase that specifically removes branching point glutamates (Fig. 6C).

Cooperative mechanism of tubulin deglutamylation

To test whether the enzymes associated with each step of the deglutamylation reaction could cooperate in the complete elimination of polyglutamate chains, we performed an *in vitro* deglutamylation assay in which we combined enzymes that shorten long glutamate chains (CCP1, CCP4 and CCP6) with CCP5 that removes branching point glutamates. As a control we also treated brain tubulin with each of the enzymes separately. In agreement with our previous observations, CCP1, CCP4 and CCP6 strongly reduced poly- but not monoglutamylation on brain tubulin, whereas CCP5 treatment resulted in a slight reduction of mono- but not polyglutamylation. However, when we treated brain tubulin with a mixture of CCP5 and either CCP1, CCP4 or CCP6, the polyglutamylation was completely eliminated and monoglutamylation was decreased to almost undetectable levels (Fig. 6D). These results clearly show that the two types of deglutamyating enzymes act in a cooperative manner and that tubulin polyglutamylation is a completely reversible posttranslational modification.

DISCUSSION

A family of enzymes catalyzing the removal of posttranslational polyglutamylation

Since the discovery that polyglutamylation is a strictly regulated posttranslational modification (Audebert et al., 1993), the identification of the enzymes involved in generation and removal of the glutamate side chains was considered as the key step towards systematic functional studies. While the glutamylating enzymes have been identified (Janke et al., 2005; van Dijk et al., 2007), the reverse enzymes have remained unknown until the very recent description of a first mammalian deglutamylase, CCP5 (Kimura et al., 2010). Here we provide evidence that in mammals, besides CCP5, three additional members of the CCP family (CCP1, CCP4 and CCP6) catalyze protein deglutamylation. We further show that the CCP deglutamylases differ in their enzymatic specificities. On highly polyglutamylated brain tubulin, CCP1, CCP4 and CCP6 catalyze the shortening of the glutamate side chains, while CCP5 exclusively removes the branching point glutamates (schematic representation: Fig. 7). A mechanism in which two types of enzymes cooperate to completely remove polyglutamylation on brain MTs is in agreement with the previous observation that deglutamylation in neurons occurs at two different rates: a fast rate for shortening of long glutamate side chains and a slower rate for the removal of branching point glutamates (Audebert et al., 1993). This differential deglutamylation might allow for a tight control over the distribution of mono- and polyglutamylation on MTs within cells or even along single MTs.

While polyglutamylation on brain MTs is mainly generated by the TLL1 polyglutamylase (Janke et al., 2005), other TLLs are responsible for polyglutamylation of other MT types. For example, TLL6 generates long side chains on axonemal MTs and plays an essential role in ciliary functions (Kubo et al., 2010; Pathak et al., 2007; Suryavanshi et al., 2010; van Dijk

et al., 2007). Strikingly, we found that CCP1 catalyzes complete removal of glutamate side chains including the branching point glutamates from MTs modified by TLL6. Since TLL1 and TLL6 both preferentially modify α -tubulin (Janke et al., 2005; van Dijk et al., 2007), this suggests that TLL6 might utilize sites on α -tubulin that are more accessible to CCP1 than the sites modified by TLL1. Thus, the use of different modification sites could be an additional parameter that regulates the dynamics of polyglutamylation and contributes to the diversity of signals generated by this modification.

CCPs also catalyze primary sequence deglutamylation

Apart from posttranslationally added glutamates, CCP1, CCP4 and CCP6 also remove gene-encoded glutamates from the C-termini of proteins. We have shown that these enzymes catalyze the removal of the C-terminal glutamate from detyrosinated tubulin, which gives rise to $\Delta 2$ -tubulin. This form of tubulin has previously been identified as a fraction of tubulin that cannot be re-tyrosinated by tubulin tyrosine ligase (TTL), and that accumulates on stable MT assemblies such as neuronal MTs (Paturle-Lafanechere et al., 1994). In addition, we demonstrate that CCP1, CCP4 and CCP6 shorten the C-terminal glutamate stretch of two important regulators of myosin functions, MLCK and telokin (Gao et al., 2001; Herring et al., 2006). Out of the eight gene-encoded glutamic acids present at the very C-termini of these proteins, seven are removed (Fig. 7). This is in agreement with previous studies, which have revealed that telokin isolated from chicken gizzard has variable number of glutamates at its C-terminus (Rusconi et al., 1997).

Our observation that additional, not yet identified, proteins undergo primary sequence deglutamylation suggests that this modification might be a general feature of proteins with multiple glutamate residues at their C-termini. Understanding the functional importance of C-terminal protein deglutamylation opens an exciting new field for future research.

Polyglutamylation is linked to neurodegeneration

Purkinje cell degeneration (pcd) mice were first described in 1976 (Mullen et al., 1976), and have since provided an excellent model to study neurodegeneration. Since the discovery that these mice lack functional CCP1 (also known as Nna1; Fernandez-Gonzalez et al., 2002), several mechanisms explaining the neurodegenerative phenotype of these mice have been proposed including lack of tubulin detyrosination, decreased protein turnover and mitochondrial defects (Berezniuk et al., 2010; Chakrabarti et al., 2010; Kalinina et al., 2007). Based on our discovery that CCP1 is a protein deglutamylase, we have demonstrated that *pcd* mice have increased levels of tubulin polyglutamylation specifically in the parts of the brain that undergo neurodegeneration, such as cerebellum and olfactory bulb. This suggested that tubulin hyperglutamylation could be the cause of neurodegeneration in the *pcd* mice, and indeed, down-regulation of the tubulin-specific neuronal polyglutamylase (TTLL1) in the cerebellum of young *pcd* mice prevented Purkinje cell death and improved motor coordination. These experiments now unambiguously demonstrate that tubulin hyperglutamylation is responsible for the Purkinje cell degeneration in the *pcd* mice.

Tubulin polyglutamylation has been proposed to regulate a number of MT functions. Recent studies have shown that polyglutamylation regulates MT-dynein interactions (Kubo et al., 2010; Suryavanshi et al., 2010) as well as spastin-mediated MT severing (Lacroix et al., 2010). Thus, it appears that tubulin hyperglutamylation could affect the interactions of MAPs and motors with the MT cytoskeleton and as a consequence lead to neurodegeneration.

Conclusion

Here we demonstrate that unlike previously suggested, CCP1 is not the long-searched-for tubulin detyrosinating enzyme, but is involved in the removal of glutamates from tubulin as well as from other substrates. By analyzing additional members of the CCP family, we have

identified a group of tubulin modifying enzymes that generate $\Delta 2$ -tubulin and that remove posttranslationally added polyglutamylation. We have also shown that the C-terminal deglutamylation of proteins is likely to be a general posttranslational modification, which might have many yet undiscovered roles in the regulation of protein functions. In addition, we found that loss of function of one of the deglutamylases in the *pcd* mice leads to MT hyperglutamylation specifically in brain regions that undergo neuronal degeneration. By depleting the tubulin-specific neuronal polyglutamylase TLL1, we were able to prevent this degeneration, thus demonstrating that MT hyperglutamylation is the primary cause of neurodegeneration in the *pcd* mice. Taken together, we have characterized a family of deglutamylating enzymes, and by analyzing the *in vivo* function of one of these deglutamylases provided evidence that the fine-tuning of the length of polyglutamate side chains on MTs is critical for neuronal function and survival.

EXPERIMENTAL PROCEDURES

Characterization of CCPs

MLCK, telokin and CCP cDNA sequences from the NCBI database or predicted for CCP4 and CCP6 were cloned into various expression plasmids after amplification from murine cDNA. Enzymatically inactive CCPs were generated by mutagenizing a conserved Zinc-binding motif (Fig. S1). CCPs fused to fluorescent proteins were expressed in cultured cells. GST-tagged MLCK and telokin were expressed in bacteria, 6His-tagged CCP1 in the baculovirus-infected insect cells, and proteins were purified by affinity. Pig brain tubulin was purified as described before (Vallee, 1986). Glutamylated tubulin was purified from HeLa cells 24 h after transfection with either TLL4 or TLL6 by affinity on a GT335-column as previously described (van Dijk et al., 2008). Enzymatic activities were determined by

incubating the extracts of CCP-expressing HEK293 cells with brain tubulin, tubulin from HeLa cells, or purified MLCK or telokin at 37°C for 6 h and analysing them by SDS-PAGE and immunoblot. For immunoprecipitation, tissue extracts were incubated with protein G coupled magnetic beads coated with anti-MLCK1 antibody, and bound proteins were analyzed by immunoblot.

Mouse experiments

Mouse experiments were performed in accordance with institutional and national regulations, and have been approved by the local ethics committee. *Pcd* mice (BALB/cByJ-*Agtpbp1*^{*pcd-3J*}-J) were obtained from The Jackson Laboratories. For tissue preparation or cell culture, mice were sacrificed and organs were quickly dissected. Control or TLL1-specific shRNA in lentivirus was injected into the left hemisphere of the cerebellum of anesthetized P10 mouse pups using a micro-pump. Mice were analyzed 30 d after injection (P40) using behavioral tests or immunohistochemistry. Sensorimotor coordination was assayed on a rotarod. Mice were trained on the rotating cylinders at constant speed (4 rpm) until they remained on the rod for 15 s, and the latency to fall from the rod was determined by accelerating the rod every 8 s by 1 rpm. Each mouse was assayed in 6 successive trials, and medians were calculated and tested using the Mann and Whitney, non-parametric *t* test.

Cell culture, immunohistochemistry and immunoblot

Cerebellar granule neuron cultures were prepared from 7 d old murine pups, cortical neuron cultures from E17.5 and MEFs from E13.5 embryos following standard procedures. HEK 293 and HeLa cell lines were grown under standard conditions. Cells were either directly analyzed by SDS-PAGE, or fixed for immunohistochemistry using standard procedures. Brain sections were permeabilized for 45 min in PBS containing 0.3% (v/v) Triton X100 and 5% (v/v) normal goat serum (NGS), washed and incubated overnight with

primary antibody. SDS-PAGE and immunoblot were performed using standard protocols. Cells, brain sections or membranes were incubated with rabbit polyE, anti-GFP, anti-GST, anti-detyrosinated tubulin or anti- $\Delta 2$ -tubulin antibodies, or mouse anti-calbindin D-28K, anti-MLCK1, GT335, 6-11B-1 and 12G10, or rat anti-tyrosinated tubulin (YL1/2) antibodies. For immunohistochemistry, anti-mouse, anti-rabbit or anti-rat antibodies conjugated with either Alexa 555 or Alexa 488, Cy3 or Cy5 fluorophores were used and nuclei were stained using either DAPI or Hoechst 33258. Fluorescent images were acquired with a LSM 710 confocal, Axioskop 50 (Carl Zeiss MicroImaging) or DMRA (Leica) microscopes, and Metamorph software. Protein bands on immunoblots were visualized with HRP-labeled donkey anti-rabbit, anti-mouse or anti-rat IgG followed by detection with chemiluminescence. For the graphical representation of modification levels in Fig. 4, protein bands from immunoblots were quantified using ImageJ software.

Database submission

Sequences for CCP4 and CCP6 have been deposited in public databases with the accession numbers FN429927 and FN427928.

References

- Audebert, S., Desbruyeres, E., Gruszczynski, C., Koulakoff, A., Gros, F., Denoulet, P., and Eddé, B. (1993). Reversible polyglutamylation of alpha- and beta-tubulin and microtubule dynamics in mouse brain neurons. *Mol Biol Cell* 4, 615-626.
- Berezniuk, I., Sironi, J., Callaway, M.B., Castro, L.M., Hirata, I.Y., Ferro, E.S., and Fricker, L.D. (2010). CCP1/Nna1 functions in protein turnover in mouse brain: Implications for cell death in Purkinje cell degeneration mice. *Faseb J.*
- Bobinnec, Y., Moudjou, M., Fouquet, J.P., Desbruyeres, E., Eddé, B., and Bornens, M. (1998). Glutamylation of centriole and cytoplasmic tubulin in proliferating non- neuronal cells. *Cell Motil Cytoskeleton* 39, 223-232.
- Bré, M.H., de Nechaud, B., Wolff, A., and Fleury, A. (1994). Glutamylated tubulin probed in ciliates with the monoclonal antibody GT335. *Cell Motil Cytoskeleton* 27, 337-349.
- Chakrabarti, L., Eng, J., Martinez, R.A., Jackson, S., Huang, J., Possin, D.E., Sopher, B.L., and La Spada, A.R. (2008). The zinc-binding domain of Nna1 is required to prevent retinal photoreceptor loss and cerebellar ataxia in Purkinje cell degeneration (pcd) mice. *Vision Res* 48, 1999-2005.
- Chakrabarti, L., Zahra, R., Jackson, S.M., Kazemi-Esfarjani, P., Sopher, B.L., Mason, A.G., Toneff, T., Ryu, S., Shaffer, S., Kansy, J.W., *et al.* (2010). Mitochondrial dysfunction in NnaD mutant flies and Purkinje cell degeneration mice reveals a role for Nna proteins in neuronal bioenergetics. *Neuron* 66, 835-847.
- Eddé, B., Rossier, J., Le Caer, J.P., Desbruyeres, E., Gros, F., and Denoulet, P. (1990). Posttranslational glutamylation of alpha-tubulin. *Science* 247, 83-85.

- Ersfeld, K., Wehland, J., Plessmann, U., Dodemont, H., Gerke, V., and Weber, K. (1993). Characterization of the tubulin-tyrosine ligase. *J Cell Biol* 120, 725-732.
- Fernandez-Gonzalez, A., La Spada, A.R., Treadaway, J., Higdon, J.C., Harris, B.S., Sidman, R.L., Morgan, J.I., and Zuo, J. (2002). Purkinje cell degeneration (pcd) phenotypes caused by mutations in the axotomy-induced gene, *Nna1*. *Science* 295, 1904-1906.
- Gao, Y., Ye, L.H., Kishi, H., Okagaki, T., Samizo, K., Nakamura, A., and Kohama, K. (2001). Myosin light chain kinase as a multifunctional regulatory protein of smooth muscle contraction. *IUBMB Life* 51, 337-344.
- Herring, B.P., El-Mounayri, O., Gallagher, P.J., Yin, F., and Zhou, J. (2006). Regulation of myosin light chain kinase and telokin expression in smooth muscle tissues. *Am J Physiol Cell Physiol* 291, C817-827.
- Ikegami, K., Sato, S., Nakamura, K., Ostrowski, L.E., and Setou, M. (2010). Tubulin polyglutamylation is essential for airway ciliary function through the regulation of beating asymmetry. *Proc Natl Acad Sci U S A* 107, 10490-10495.
- Janke, C., Rogowski, K., Wloga, D., Regnard, C., Kajava, A.V., Strub, J.-M., Temurak, N., van Dijk, J., Boucher, D., van Dorsselaer, A., et al. (2005). Tubulin polyglutamylase enzymes are members of the TTL domain protein family. *Science* 308, 1758-1762.
- Kalinina, E., Biswas, R., Berezniuk, I., Hermoso, A., Aviles, F.X., and Fricker, L.D. (2007). A novel subfamily of mouse cytosolic carboxypeptidases. *Faseb J* 21, 836-850.
- Kimura, Y., Kurabe, N., Ikegami, K., Tsutsumi, K., Konishi, Y., Kaplan, O.I., Kunitomo, H., Iino, Y., Blacque, O.E., and Setou, M. (2010). Identification of tubulin deglutamylase among *Caenorhabditis elegans* and mammalian cytosolic carboxypeptidases (CCPs). *J Biol Chem* 285, 22936-22941.

- Kubo, T., Yanagisawa, H.-a., Yagi, T., Hirono, M., and Kamiya, R. (2010). Tubulin polyglutamylation regulates axonemal motility by modulating activities of inner-arm dyneins. *Curr Biol* 20, 441-445.
- Lacroix, B., van Dijk, J., Gold, N.D., Guizetti, J., Aldrian-Herrada, G., Rogowski, K., Gerlich, D.W., and Janke, C. (2010). Tubulin polyglutamylation stimulates spastin-mediated microtubule severing. *J Cell Biol* 189, 945-954.
- Mullen, R.J., Eicher, E.M., and Sidman, R.L. (1976). Purkinje cell degeneration, a new neurological mutation in the mouse. *Proc Natl Acad Sci U S A* 73, 208-212.
- Pathak, N., Obara, T., Mangos, S., Liu, Y., and Drummond, I.A. (2007). The Zebrafish floor Gene Encodes an Essential Regulator of Cilia Tubulin Polyglutamylation. *Mol Biol Cell* 18, 4353-4364.
- Paturle-Lafanechere, L., Eddé, B., Denoulet, P., Van Dorsselaer, A., Mazarguil, H., Le Caer, J.P., Wehland, J., and Job, D. (1991). Characterization of a major brain tubulin variant which cannot be tyrosinated. *Biochemistry* 30, 10523-10528.
- Paturle-Lafanechere, L., Manier, M., Trigault, N., Pirollet, F., Mazarguil, H., and Job, D. (1994). Accumulation of delta 2-tubulin, a major tubulin variant that cannot be tyrosinated, in neuronal tissues and in stable microtubule assemblies. *J Cell Sci* 107, 1529-1543.
- Redeker, V., Frankfurter, A., Parker, S.K., Rossier, J., and Detrich, H.W., 3rd (2004). Posttranslational modification of brain tubulins from the antarctic fish *Notothenia coriiceps*: reduced C-terminal glutamylation correlates with efficient microtubule assembly at low temperature. *Biochemistry* 43, 12265-12274.
- Regnard, C., Desbruyeres, E., Denoulet, P., and Eddé, B. (1999). Tubulin polyglutamylase: isozymic variants and regulation during the cell cycle in HeLa cells. *J Cell Sci* 112, 4281-4289.

- Regnard, C., Desbruyeres, E., Huet, J.C., Beauvallet, C., Pernollet, J.C., and Eddé, B. (2000). Polyglutamylation of nucleosome assembly proteins. *J Biol Chem* 275, 15969-15976.
- Rodriguez de la Vega, M., Sevilla, R.G., Hermoso, A., Lorenzo, J., Tanco, S., Diez, A., Fricker, L.D., Bautista, J.M., and Aviles, F.X. (2007). Nna1-like proteins are active metallopeptidases of a new and diverse M14 subfamily. *Faseb J* 21, 851-865.
- Rüdiger, M., Plessman, U., Kloppel, K.D., Wehland, J., and Weber, K. (1992). Class II tubulin, the major brain beta tubulin isotype is polyglutamylated on glutamic acid residue 435. *FEBS Lett* 308, 101-105.
- Rusconi, F., Potier, M.C., Le Caer, J.P., Schmitter, J.M., and Rossier, J. (1997). Characterization of the chicken telokin heterogeneity by time-of-flight mass spectrometry. *Biochemistry* 36, 11021-11026.
- Smith, A.F., Bigsby, R.M., Word, R.A., and Herring, B.P. (1998). A 310-bp minimal promoter mediates smooth muscle cell-specific expression of telokin. *Am J Physiol* 274, C1188-1195; discussion C1187.
- Suryavanshi, S., Edde, B., Fox, L.A., Guerrero, S., Hard, R., Hennessey, T., Kabi, A., Malison, D., Pennock, D., Sale, W.S., et al. (2010). Tubulin glutamylation regulates ciliary motility by altering inner dynein arm activity. *Curr Biol* 20, 435-440.
- Vallee, R.B. (1986). Reversible assembly purification of microtubules without assembly-promoting agents and further purification of tubulin, microtubule-associated proteins, and MAP fragments. *Methods Enzymol* 134, 89-104.
- van Dijk, J., Miro, J., Strub, J.-M., Lacroix, B., van Dorsselaer, A., Eddé, B., and Janke, C. (2008). Polyglutamylation Is a Post-translational Modification with a Broad Range of Substrates. *J Biol Chem* 283, 3915-3922.

- van Dijk, J., Rogowski, K., Miro, J., Lacroix, B., Eddé, B., and Janke, C. (2007). A targeted multienzyme mechanism for selective microtubule polyglutamylation. *Mol Cell* 26, 437-448.
- Wang, T., and Morgan, J.I. (2007). The Purkinje cell degeneration (pcd) mouse: an unexpected molecular link between neuronal degeneration and regeneration. *Brain Res* 1140, 26-40.
- Wang, T., Parris, J., Li, L., and Morgan, J.I. (2006). The carboxypeptidase-like substrate-binding site in Nna1 is essential for the rescue of the Purkinje cell degeneration (pcd) phenotype. *Mol Cell Neurosci* 33, 200-213.
- Wloga, D., Dave, D., Meagley, J., Rogowski, K., Jerka-Dziadosz, M., and Gaertig, J. (2009). Hyperglutamylation of tubulin can either stabilize or destabilize microtubules in the same cell. *Eukaryot Cell*.
- Wolff, A., de Nechaud, B., Chillet, D., Mazarguil, H., Desbruyeres, E., Audebert, S., Eddé, B., Gros, F., and Denoulet, P. (1992). Distribution of glutamylated alpha and beta-tubulin in mouse tissues using a specific monoclonal antibody, GT335. *Eur J Cell Biol* 59, 425-432.

Acknowledgements:

This work was supported by the CNRS, the Universities Montpellier 2 and 1, the Institut Curie, the Association pour la Recherche sur le Cancer (ARC) award 3140 to CJ and 4892 and 7927 to AA, the French National Research Agency (ANR) awards 05-JCJC-0035 and 08-JCJC-0007 to CJ, and “TyrTips” to AA, the Fondation pour la Recherche Médicale (FRM) research grant DEQ20081213977, the HFSP program grant RGP 23/2008 and the EMBO Young Investigator Program grant to CJ, the La Ligue contre le cancer research grant R07Job to AA and the Alzheimer Forschung Initiative project 06825 to MH. BL was supported by a fellowship from the La Ligue contre le Cancer, and the EMBO short-term fellowship ASTF 157-2007. KR received two postdoctoral fellowships from the La Ligue contre le Cancer and the EMBO long-term fellowship ALTF 546-2006.

We thank L. Cotter (INSERM U836, Grenoble, France), G. Aldrian-Herrada, J. Boudeau, J.-M. Donnay, J.-C. Mazur, J. Miro (CRBM, Montpellier, France), K. Chebli, C. Jacquet, E. Jouffre (IGMM, Montpellier, France), C. Alberti, E. Belloir, H. Yu (Institut Curie, Orsay, France), V. Bäcker, J. Cau, S. DeRossi, P. Travo (RIO Imaging facility at the CRBM) and R. Holzer (University of Leipzig, Germany) for technical assistance. We are grateful to D. Job (INSERM U836, Grenoble, France) and U. Schmidt (IGMM, Montpellier, France) for instructive discussions. We are grateful to L. Lafanechère (CEA, Grenoble, France) for the kind gift of the anti- $\Delta 2$ -tubulin antibody. The monoclonal antibody 12G10 developed by J. Frankel and M. Nelson was obtained from the Developmental Studies Hybridoma Bank developed under the auspices of the NICHD and maintained by the University of Iowa.

The authors declare no competing financial interests.

Figure legends

Figure 1 Enzymatic characterization of CCP1

(A) Immunoblot of protein extracts from HEK293 cells expressing active (EYFP-CCP1) or inactive (EYFP-CCP1d) CCP1. (B) Immunofluorescence of mouse embryonic fibroblasts (MEFs) expressing EGFP-CCP1. Anti- $\Delta 2$ -tubulin antibody specifically labels the cell expressing EGFP-CCP1. (C) Immunofluorescence of mouse hippocampal neurons expressing EGFP-CCP1. (D) Immunoblot of tubulin treated with extracts from HEK293 cell expressing either active or inactive EYFP-CCP1. Three types of tubulin were used: brain tubulin, and HeLa tubulin modified with TLL4 or TLL6. TLL4 does not generate a polyE signal on tubulin (not shown) (E) Immunoblot of protein extracts prepared from HEK293 cells co-expressing TLL4-EYFP or TLL6-EYFP together with active or inactive EYFP-CCP1. Note that the GT335 signal generated by TLL4 is not removed by CCP1, while TLL6-dependent GT335 labeling on tubulin and TLL6 is reduced by CCP1. Scale bars in (B) and (C) are 20 μ m. See also Fig. S2.

Figure 2 Characterization of CCP1 substrates

(A) Comparative immunoblot of protein extracts prepared from organs of WT and *pcd* mice. Whole-tissue extracts were tested with anti-tyr-tubulin, detyr-tubulin, $\Delta 2$ -tubulin and polyE. Note the disappearance of anti- $\Delta 2$ -tubulin and anti-detyr-tubulin labeling and increase in polyE staining for 130 kDa substrate in the extracts from stomach and uterus of the *pcd* mice. (B) Immunoprecipitations with anti-MLCK1 antibodies using protein extracts from stomach and uterus of WT mice. The fractions were tested in immunoblot. In the bound fraction, protein bands of the same size are detected with anti- $\Delta 2$ -tubulin and anti-MLCK1 antibodies. (*degradation product) (C) Immunoblot of protein extracts prepared from HEK293 cells co-expressing EYFP-CCP1 or EYFP-CCP1d together with EYFP-MLCK1 or

EYFP-telokin. The $\Delta 2$ -tubulin labeling correlates with the expression of active CCP1, and polyE labeling correlates with the expression of inactive CCP1. **(D)** *In vitro* deglutamylation assay with purified GST-telokin and 6His-CCP1. GST-telokin and 6His-CCP1 were incubated in the presence or absence of phenanthroline. GST-telokin is specifically detected with $\Delta 2$ -tubulin antibody after incubation with 6His-CCP1. In the presence of phenanthroline, telokin remains in the polyE-reactive form and is not detected by anti- $\Delta 2$ -tubulin antibody. **(E)** Immunoblot of protein extract from HEK293 cells co-expressing EYFP-CCP1 and different artificial substrates based on EYFP-telokin. The sequence of the C-terminal tails of the telokin-like substrates is indicated starting from glycine 151. Only WT telokin (-GEEEEEEEE) co-expressed with CCP1 is labeled by anti- $\Delta 2$ -tubulin antibody. See also Fig. S4C and Tables S1-4.

Figure 3 Enzymatic characterization of CCP4 and CCP6

(A) Immunofluorescence of MEFs expressing either EGFP-CCP4 or EGFP-CCP6. Scale bar is 20 μ m. **(B, C)** Immunoblot of brain tubulin treated with protein extracts from HEK293 cells expressing **(B)** active or inactive EGFP-CCP4 and **(C)** active or inactive EGFP-CCP6. Note the specific reduction of polyE signal after the treatment with active CCP4 or CCP6. See also Fig. S3, S4A, B.

Figure 4 Analysis of tubulin modifications in different brain regions of the *pcd* mice

(A) Immunoblot of protein extracts prepared from cerebellum and cerebral cortex of wild type (WT) and *pcd* mice at different stages of brain development (postnatal days 7, 14, 21 and adult animals). **(B)** Graphical representation of antibody signals detected in (A). The plotted values represent the relative intensities of the immunoblots of *pcd* samples (WT=100%) after normalization to total tubulin levels (12G10). **(C)** Immunoblot of protein extracts from cerebellar granule neurons (CGNs) isolated at postnatal day 7 (P7) or cortical neurons isolated

at embryonic day 17 (E17) and cultured for 7 days (7DIV). **(D)** Graphical representation of modification levels in *pcd* versus WT neurons. Relative intensities were calculated as in (B). **(E)** Immunoblot of protein extracts from olfactory bulb of adult mice. **(F)** Graphical representation of modification levels in *pcd* versus WT samples. Relative intensities were calculated as in (B). See also Fig. S5

Figure 5 Rescue of Purkinje cell degeneration by TTLL1-depletion

(A) Immunohistochemistry of thin cerebellar sections of WT or *pcd* mice injected with lentivirus expressing either GFP (control) or GFP and shTTLL1 (Fig. S6). Purkinje cells are visualized with anti-calbindin D antibody, and the GFP signal was amplified using an anti-GFP antibody. In the panels that represent the *pcd* cerebella, only the left-hand sides of the lobes were infected by the virus (GFP). In control-injected *pcd* brains, Purkinje cells are mostly absent; while in shTTLL1-infected *pcd* brains, Purkinje cells survive. Note that GFP expression in Purkinje cells is clearly visible only at higher magnification (see panel B). Scale bar is 100 μm . **(B)** Morphology of Purkinje cells from cerebella treated as in (A). Purkinje cells from WT brains infected with control virus show a typical highly complex dendritic tree. Note that only few Purkinje cells are infected (GFP-positive). In *pcd* mice, Purkinje cells survive rarely and show abnormal morphology (panel “non-infected”). In contrast, *pcd* Purkinje cells infected with shTTLL1 virus survived and showed normal morphology. Scale bar is 20 μm **(C)** Rotarod behavioral test of control and shTTLL1 virus-injected *pcd* mice at P40 (30 d after virus injection). The graphics represent median values with 25th-75th percentiles boxes and whiskers corresponding to the minimal and maximal values. shTTLL1-injected *pcd* mice remained significantly longer on the rotating cylinder than control-injected mice (* $p < 0.05$; Mann and Whitney, non parametric t test, $n=4$). See also Fig. S6.

Figure 6 Enzymatic characterization of CCP5 and the two-step deglutamylation mechanism

(A) Immunofluorescence of U2OS cells co-expressing TTLL4-EYFP and either active or inactive CCP5-ECFP. The TTLL4-dependent GT335 labeling of MTs is completely blocked by co-expression with active CCP5. (B) Immunoblot of protein extracts from HEK293 cells co-expressing TTLL4-EYFP or TTLL6-EYFP with active or inactive CCP5-EYFP. No GT335 signal is detected after co-expression of active CCP5 and TTLL4. The GT335 and the polyE signal are strongly diminished on tubulin after co-expression of TTLL6 and active CCP5, while the polyE signal on TTLL6 remains unchanged. (C) Immunoblot of tubulin treated with HEK293 cell extracts after expression of either active or inactive EYFP-CCP5. Three types of tubulin were used: brain tubulin, and HeLa tubulin modified with TTLL4 or TTLL6. TTLL4-modified tubulin is not labeled with polyE (not shown). (D) Immunoblot of brain tubulin treated with cell extracts containing each of the four CCPs or combinations of CCP5-EYFP with EYFP-CCP1, or EGFP-CCP4, or EGFP-CCP6. Combinations of CCP5 and side-chain shortening enzymes leads to the removal of both, polyE and GT335 signal from brain tubulin. (* degradation product of EYFP-CCP1)

Figure 7 The enzymatic mechanism of protein deglutamylation

Schematic representation of the deglutamylation reactions catalyzed by CCP1, CCP4, CCP5 and CCP6 on brain tubulin (A) and MLCK (B; the C-terminal sequences of murine α 1-tubulin and MLCK1 are represented). (A) CCP1, CCP4 and CCP6 shorten the long glutamate chains generated by posttranslational polyglutamylation and subsequently, CCP5 removes the branching point glutamate. They also catalyze the formation of Δ 2-tubulin, which requires prior detyrosination. (B) The C-terminal stretch of glutamate residues of MLCK1 is shortened to one glutamate by CCP1, CCP4 or CCP6. (A, B) The epitopes recognized by modification-specific antibodies are indicated (*italic*).

Figure 1[Click here to download Figure: Rogowski_Fig1.pdf](#)

Rogowski et al., Figure 1

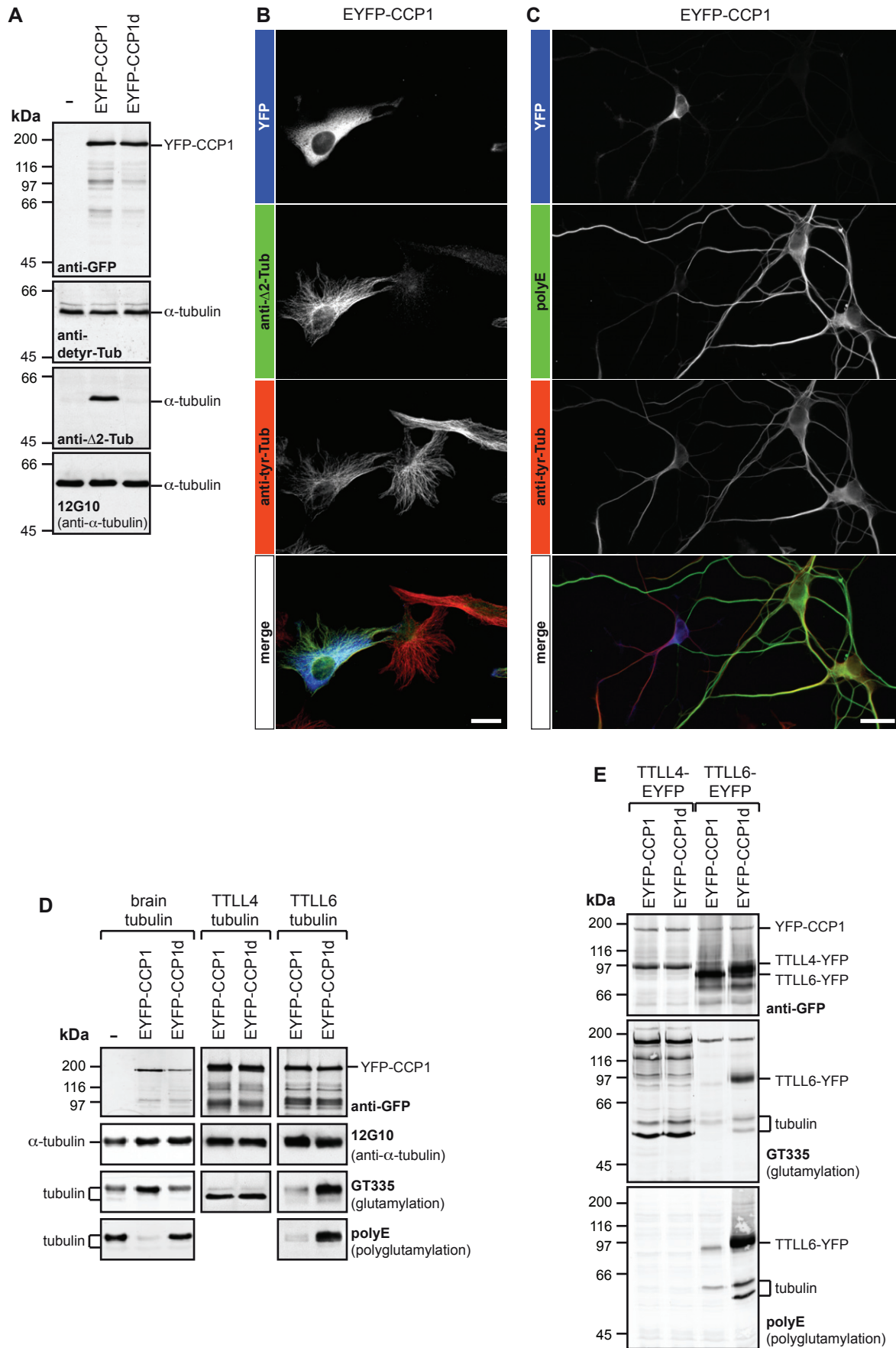
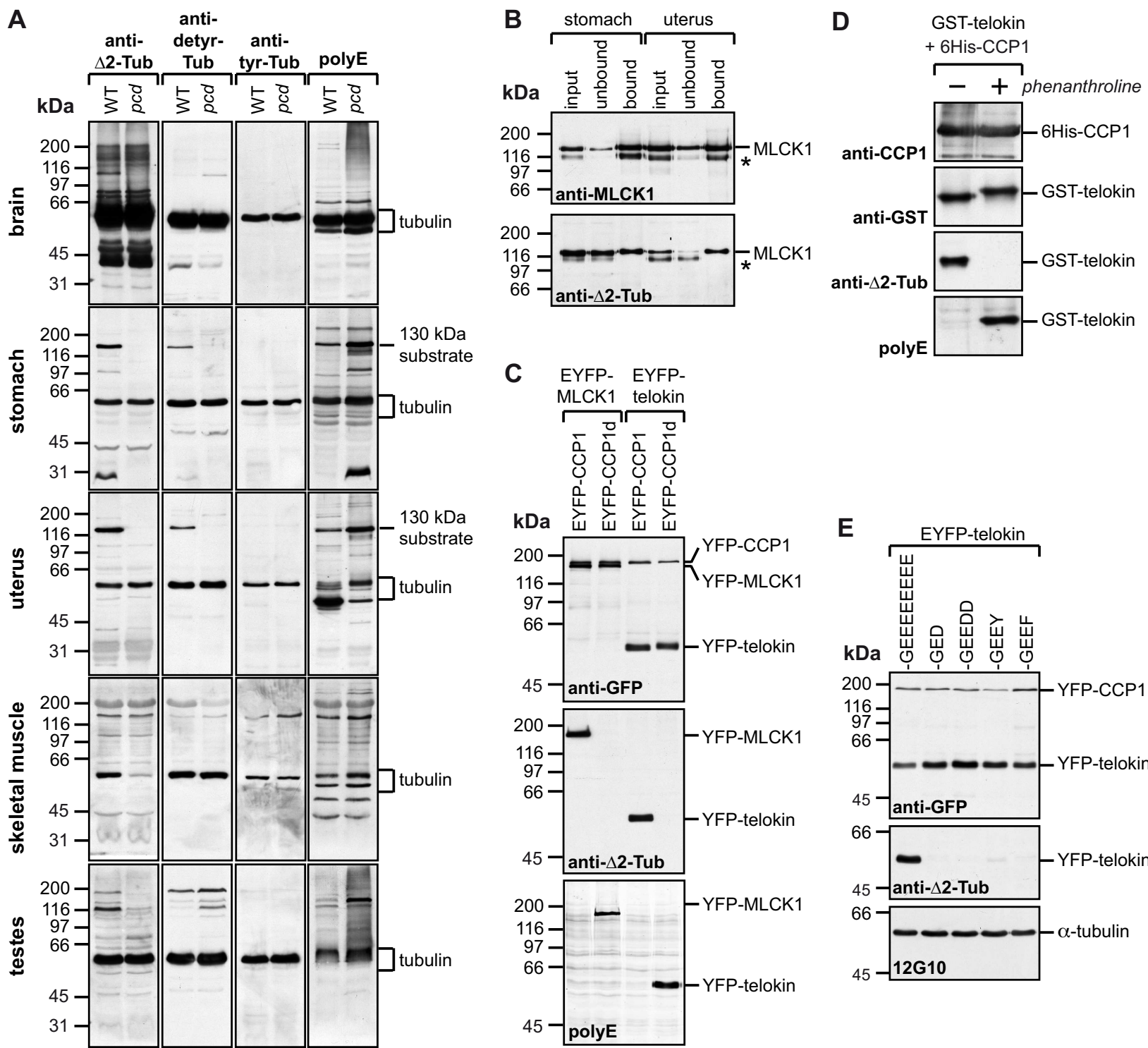


Figure 2
[Click here to download Figure: Rogowski_Fig2.eps](#)

Rogowski et al., Figure 2



Rogowski et al., Figure 3

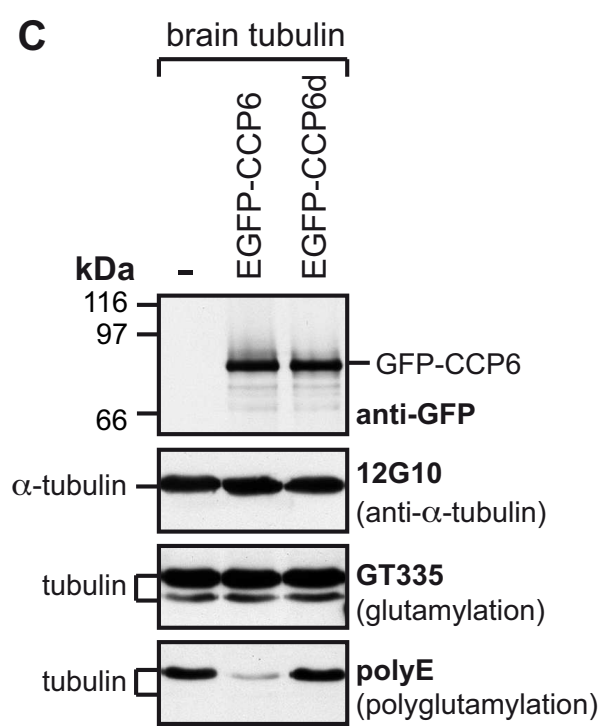
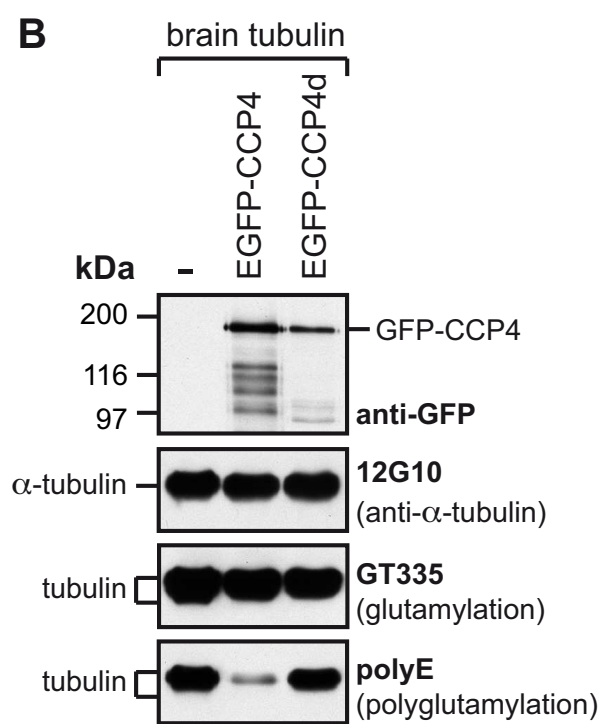
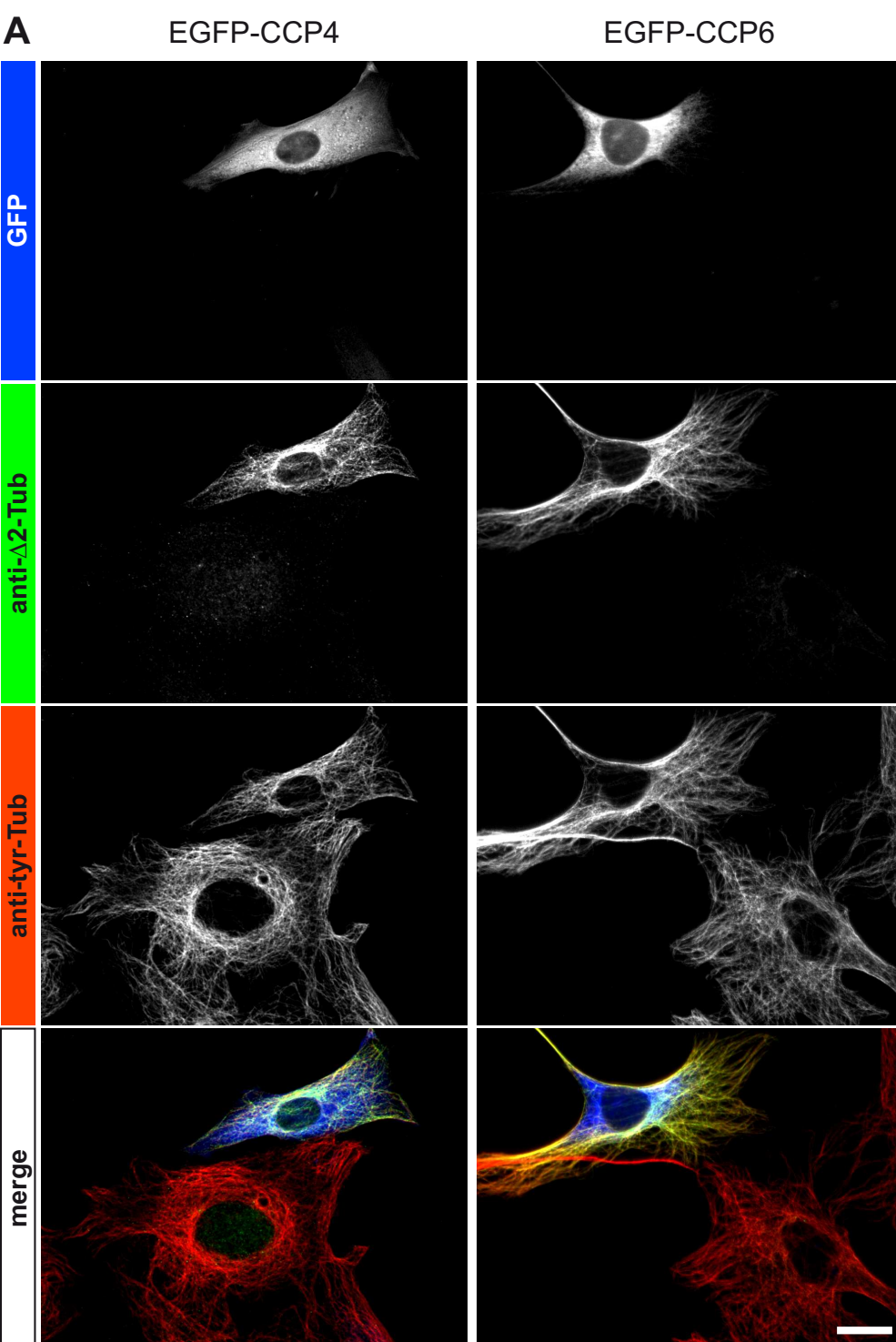


Figure 4
[Click here to download Figure: Rogowski_Fig4.eps](#)

Rogowski et al., Figure 4

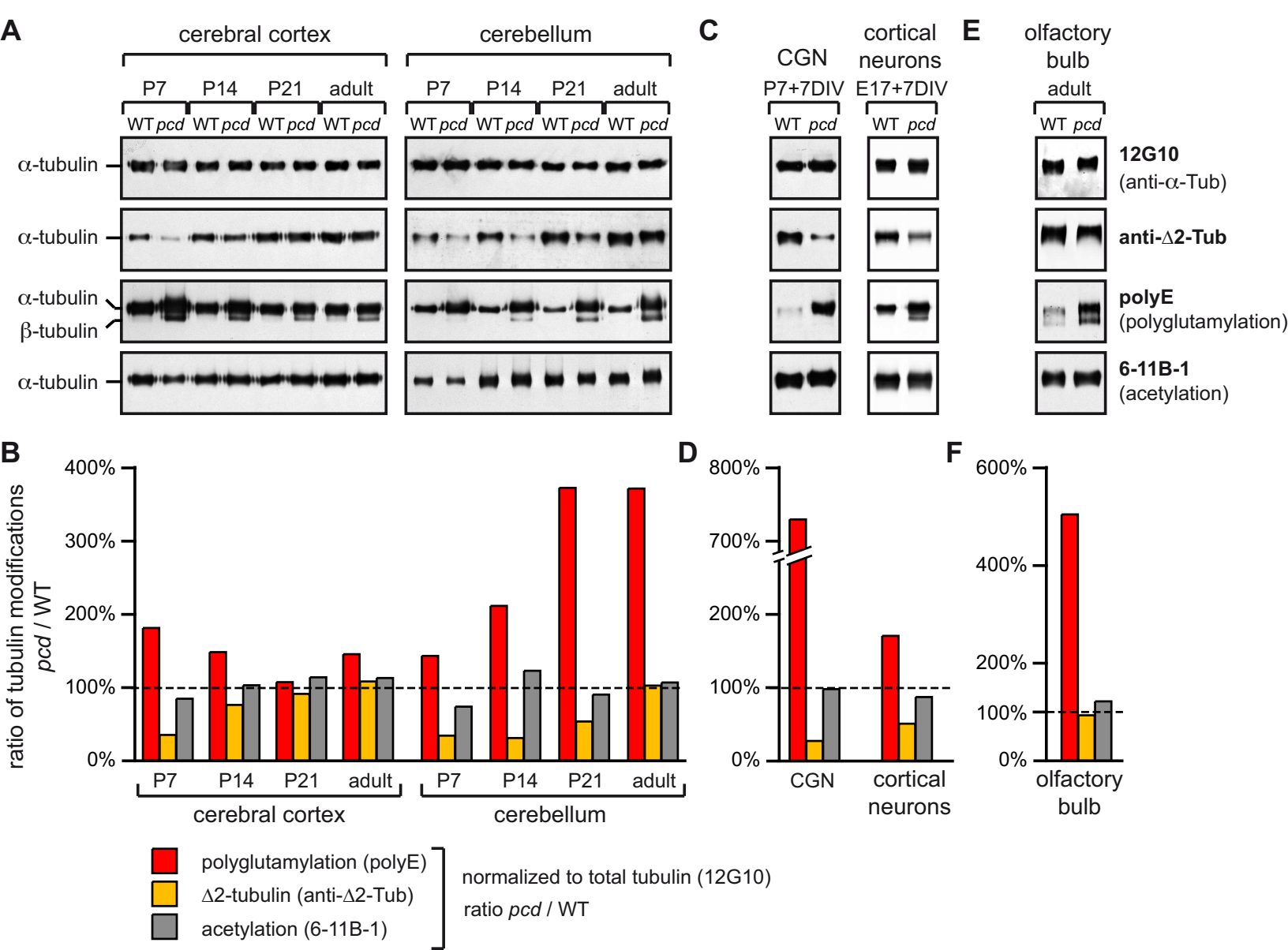
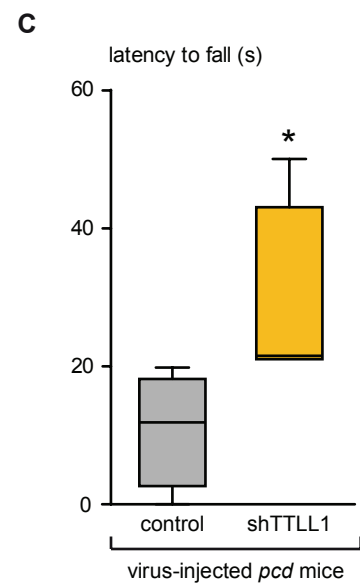
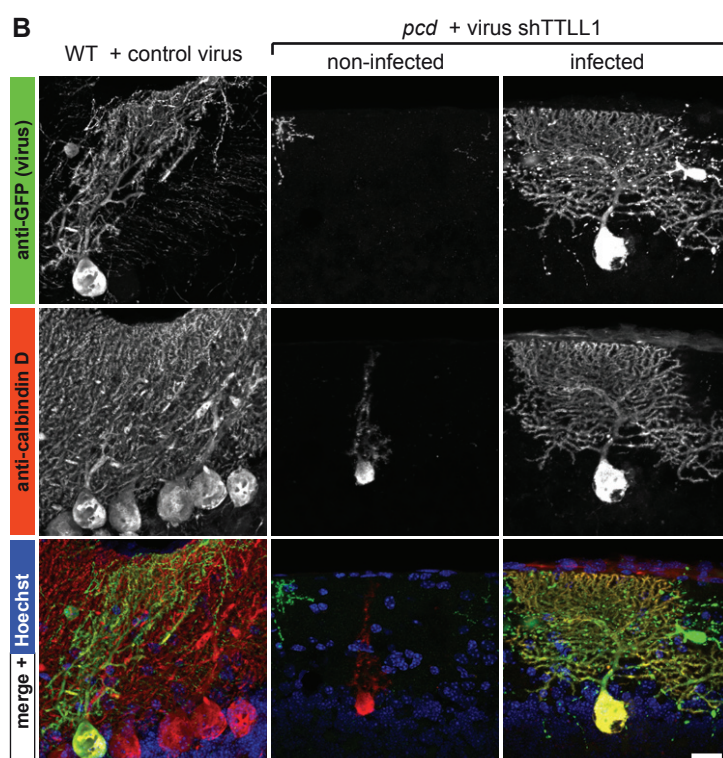
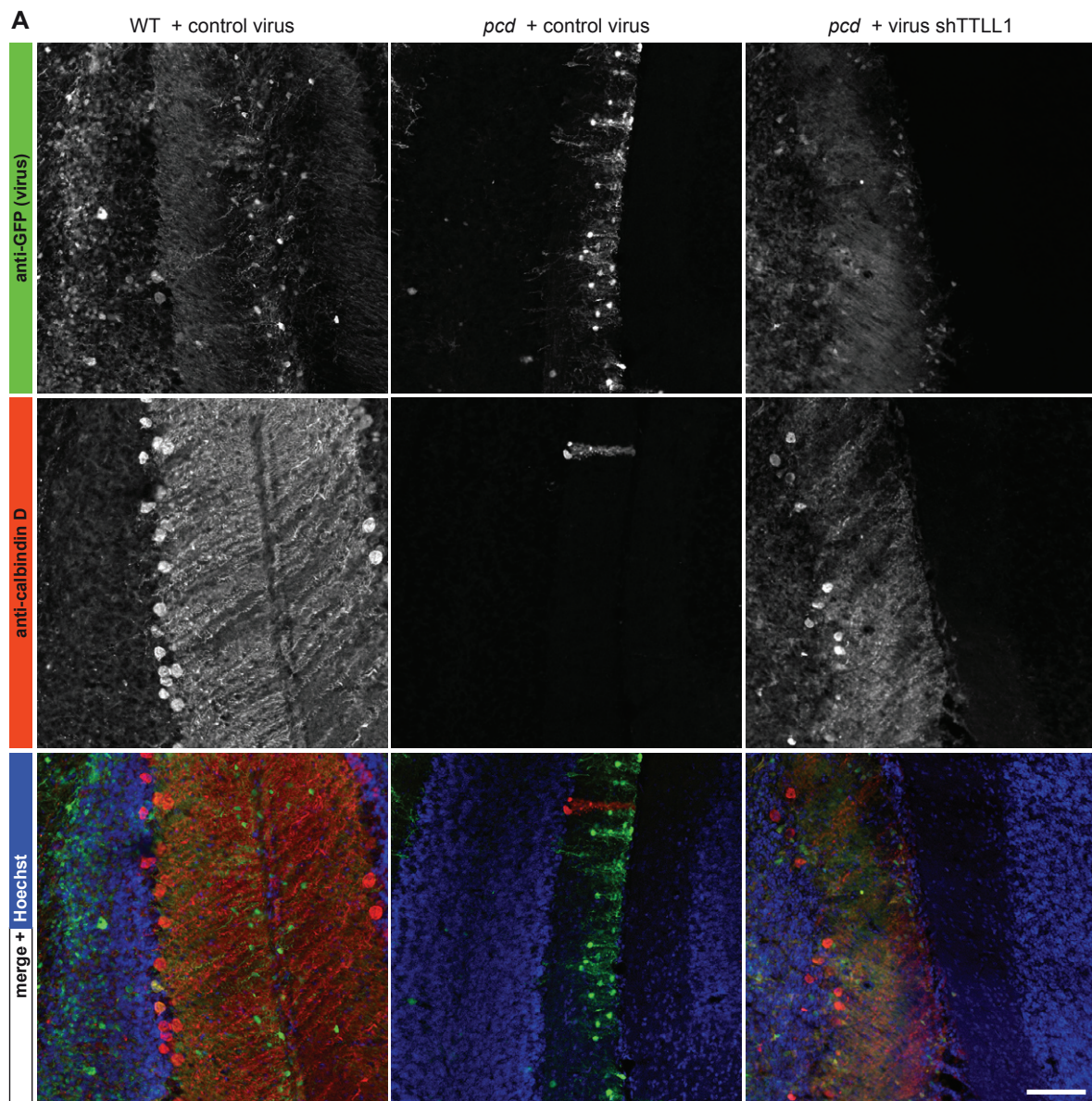


Figure 5
[Click here to download Figure: Rogowski_Fig5.pdf](#)
 Rogowski et al., Figure 5



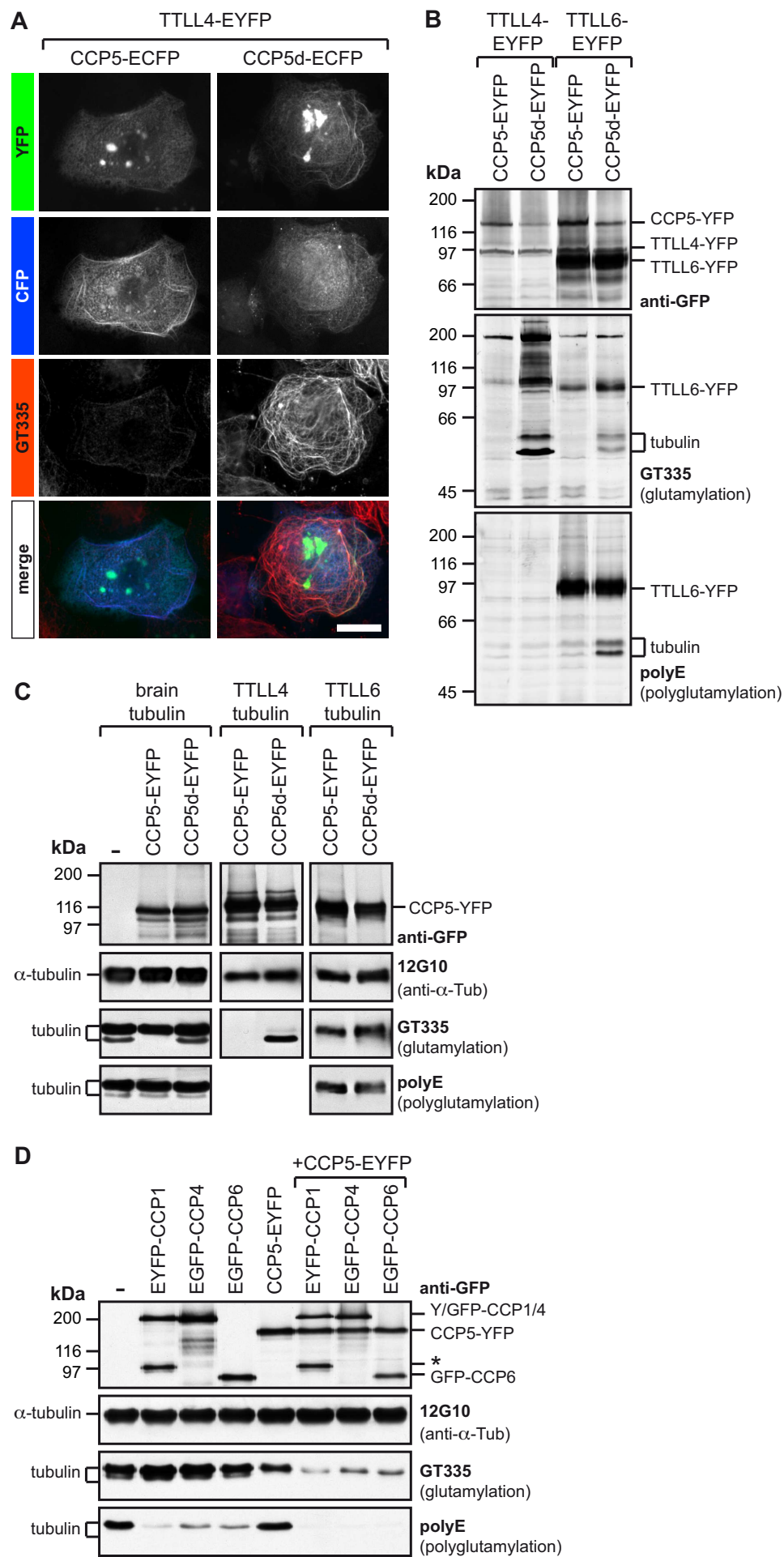
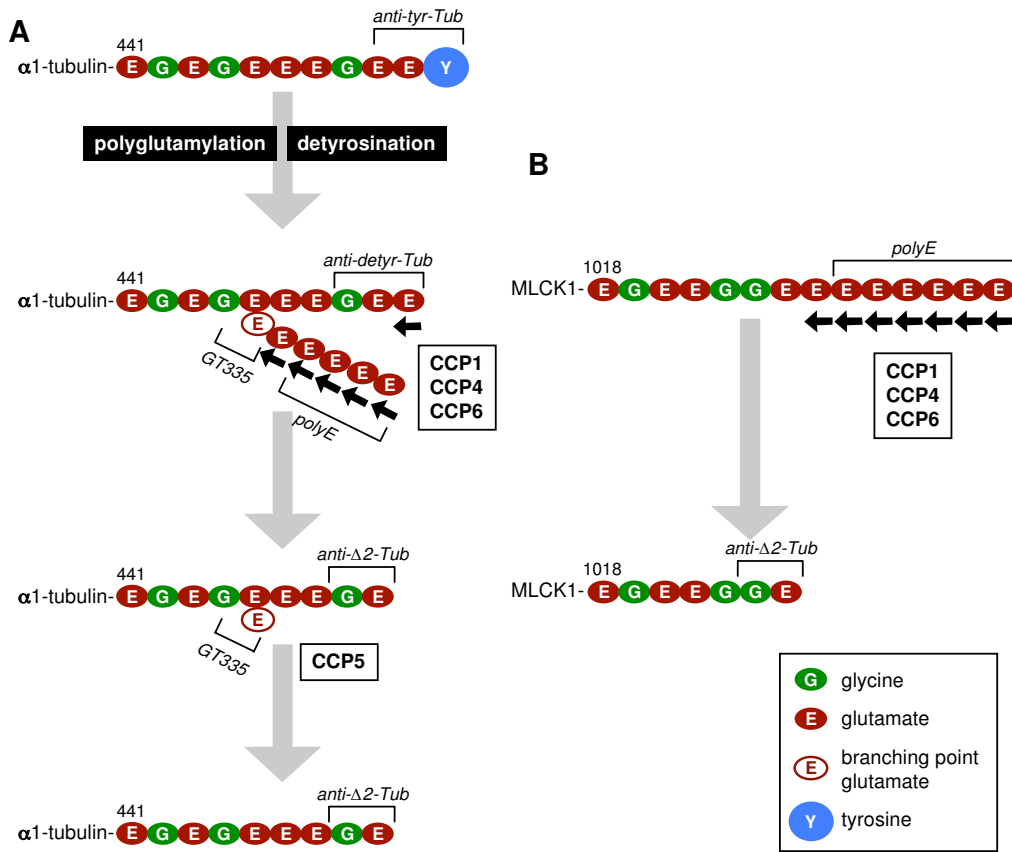


Figure 7
[Click here to download Figure: Rogowski_Fig7.eps](#)

Rogowski et al., Figure 7



Inventory of supplementary online material for Rogowski et al.

1. Figure S1 CCP sequence alignment (related to Fig. 1, 3, 6, S2, S3, S4)
2. Figure S2 Further characterization of CCP1 (related to Fig. 1)
3. Figure S3: Further characterization of CCP4 and CCP6 (related to Fig. 3)
4. Figure S4 Deglutamylation of MLCK1 and telokin (related to Fig. 2, 3)
5. Figure S5: Immunohistochemical and PCR analysis of pcd mice (related to Fig. 4)
6. Figure S6: Test of anti-TTLL1 shRNA efficiency (related to Fig. 5)
7. Table S1: Summary of proteins identified in the anti- $\Delta 2$ -tubulin reactive 130 kDa protein band from stomach (related to Fig. 2)
8. Table S2: Complete mass spectrometry data on the analysis of the anti- $\Delta 2$ -tubulin reactive 130 kDa protein band from stomach (related to Fig. 2 and Table S1); presented as additional Excel file Rogowski_TableS2
9. Table S3: Summary of proteins identified in the anti- $\Delta 2$ -tubulin reactive 20 kDa protein band from stomach (related to Fig. 2)
10. Table S4: Complete mass spectrometry data on the analysis of the anti- $\Delta 2$ -tubulin reactive 20 kDa protein band from stomach (related to Fig. 2 and Table S3) presented as additional Excel file Rogowski_TableS4
11. Detailed experimental procedures: detailed description of all experimental procedures used in this study
12. Supplementary references

Supplementary online material for Rogowski et al.

Supplementary data

```

CCP1 631 SVPEYSEVAYPDYFCHIPFPFKEPIERPYPVORTKTAODIERLIHQNDIDRVVYDLDNPTYYTTPPEGDTLKENSKFESGNLRKVIQIR
CCP2 178 EIVGEEQCTVVVQOLDSVPAEGTYFTSSRI GGRGTIKELAVTLQGP-----DDNTLLFESRFESGNLQKAVRVG
CCP3 123 EVYPNSKEDTVVVLAEADAYKEP-CFVYSRVGGARTSLKQPV DNC-----DNTLVEEARFESGNLQKAVKVA
CCP4 522 SAVGFKTMFPDLWCHCPFPAAQPMIDRKLGVORIKLLEDIRRLHPSDVINKVVFSLDEPRPLOGSISNCLMEHSEKFFESGNLRKAVQVR
CCP5 39 ATAPASG-----SAASP
CCP6 39 EKK-----GHLTFACFESGNLRVVEQVS

CCP1 721 KSEYDLIINSDINSNHYH---QWFYFEVSGMRPFGVAVRFNIINCEKSNSSQENYGMQPLMYSVOEALNAREWWRMGTDICYYKNHFSRS
CCP2 248 IYVEYELTERTDLYIDKKEIT---QWFYFRVQNTKRDATYREFTLVNLLKPKSLYAVGMKPLMYSQOLDATIYNICWRREGRREIKYYKNNV---
CCP3 188 DHEYELTVRPDLEFNKKEIT---QWYFQVQNTQAEIVMREFTLVNFTKPKASLYNRMGMKPLFYSEKEAKTHNICWORIGDQIKYYKNNL---
CCP4 612 EFEYDLLVADVNSSQEQ---QWFYFKVSGMRAAVPMHFNIINCEKPNSSQENYGMQPLMYSVKEALLGRPAWIFRTGSDICYYKNHYRQN
CCP5 51 DYEENVWTRPDCAETEVENGNRSWYFYSVRGGTFCKLIRKINIMNMKQSKLYSQGMAPFVR---LPSRERWERIRERPT EMT-----
CCP6 63 DFEYDLFTRPDCNPRFR---VWENFIVENVELQRVIFNIVNFSKTKSLYRDGMAPMVKS---TS-REKWRQLPPKNVYYR-----

CCP1 807 SVAAGGQKCKSVYITITFTVNFPHKQ-DVCYFAYHYPTYSTLQMHQOKLES-----AHNPOQLYFRKDVLCETLSEGNICPLVTTITA
CCP2 331 -----DDGOQLYCLTWTTFPHDQ-DTCFFAHYHYPTYTDLQCYLLSVAN-----NP-TQSFCLRALGRSLAGNIVYLLTITN
CCP3 271 -----GQDCRHFFSLTWTTFPHSQ-DTCYFAHCYPTYSTLQEYLSGINS-----DP-VRSKFCIRVLCHTLARNVYVLLTITT
CCP4 698 AATMDCALCKRYITLTAVTFPHNE-DACYLAFHYPTYSTLMTHEILER-----SIDHRETYFRHDVLCQTLGGNCPCLVTTITA
CCP5 132 -----ETQSVLSEVHRFVEGRGATTEFAFCYPFYSYDCQDLSQLQRFSENYSYTHSSPLDSIYYHRELLCYSLDGLRVDLLTITS
CCP6 139 -----CPDHRKNVMSBAFCEDRED-DIYCFAYCYPTYTRQHYLDSLQK-----KN-MDYFER--EQLGQSQOROEDLLTITS

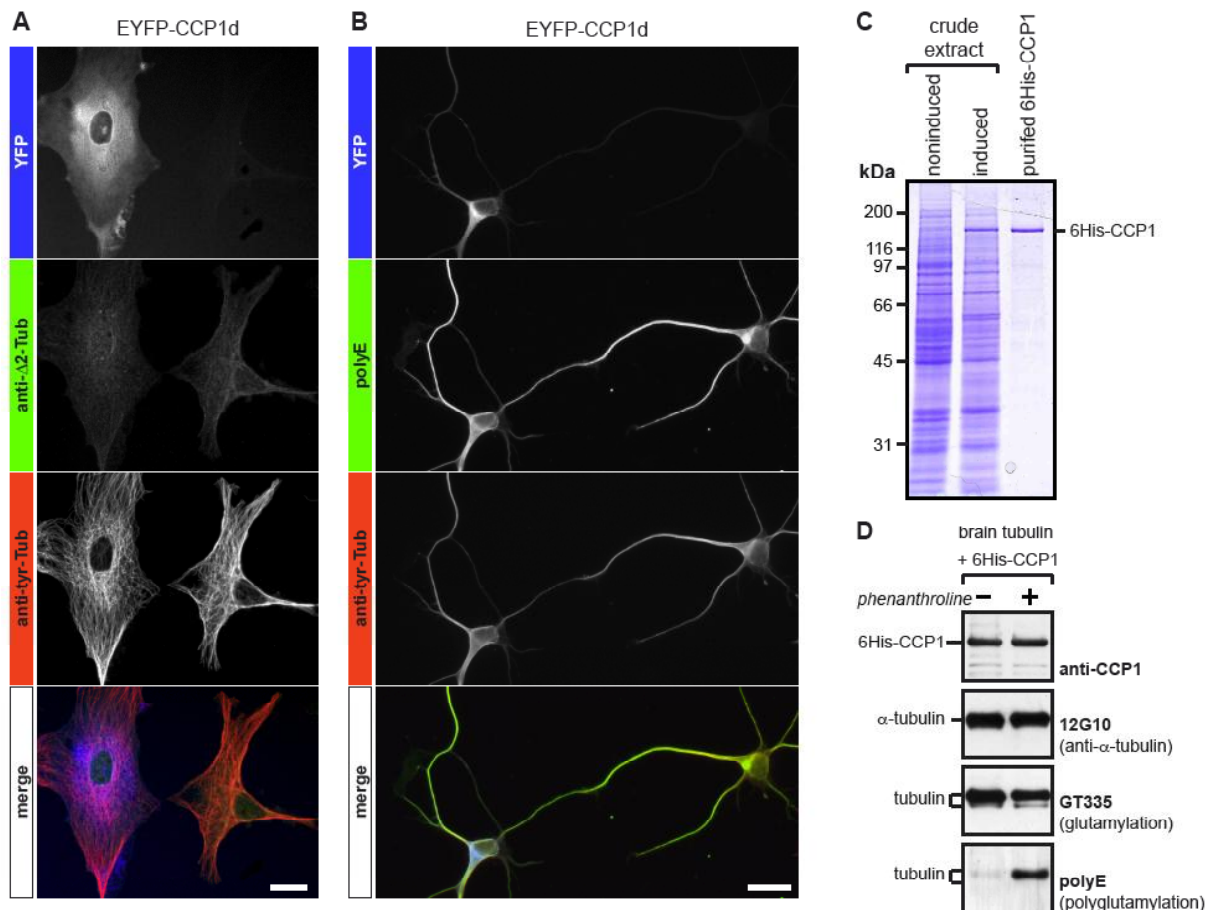
CCP1 887 MPEENY-----YEHICQERTFPYFEL SARVHPGETNASWVMKGTLEYLMS-NSETAQSLRPSYIFKIVPMLNPDGVINGNH
CCP2 405 ESRTP-----QEAAAANKAVLSARVHPGESNSSWIMNGFLDFILS-NSEDAQLLRDIFVFKVIPMLNPDGVIVGNY
CCP3 345 ELKQ-----SDSKKAVILTARVHPGETNSWIMKGFLDYILG-DSSDARLLRDTFIFKVVVPMNPDGVIVGNY
CCP4 778 FPEENS-----TEHLEQRCFPYQVITARVHPGESNASWVMKGTLEFLVS-SDEVARLLRENFVFKIIPMLNPDGVINGNH
CCP5 213 CHGLRDDRPRLEQLFPDLGTRPFRFETGRIEFLSARVHPGETPSSFVNGFLDFILRPPDDEPRAQTLRLRFVFKIIPMLNPDGVIRGHY
CCP6 211 BENLR-----EGSEKVKLEITGRVHPGETPSSFVCGIIFDFLVS-CHETARVLRREHLVFKIAPMLNPDGVIVGNY

CCP1 962 RCSLSGEDLNROQSENP ELHPTIYHAKGLLOYLAA-V-----
CCP2 475 RCSLACRDLNRHAKIVLKDSEFCIYTRKMIKRLE-----
CCP3 413 RCSLACRDLNRNYTSLKESFESVYTRNMINRLME-----
CCP4 853 RCSLRGEEDLNROHLSPOAHLQPTIYHAKGLLHYLSS-T-----
CCP5 303 RTDSRQVNLNRQVLLKPDVAVLHPATYCAKAVLIVHVSRLNAKSPTNQOPTLHLPEAPLSLEKANNLHNEAHLGQSPDGENPATWPET
CCP6 280 RCSLMGEEDLNRRHLDLSPWAHPTLHGVKQLIIRKLYNDP-----

```

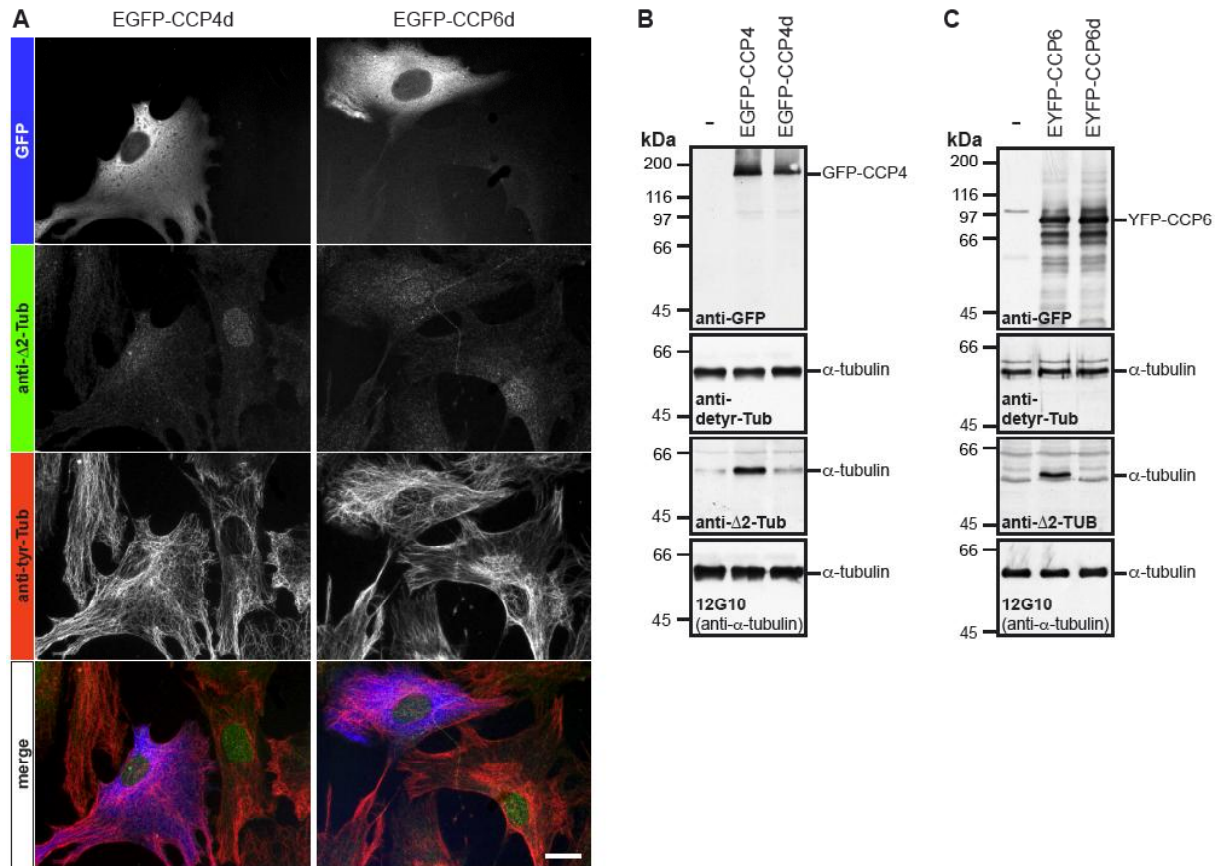
Supplementary Figure S1 CCP sequence alignment (related to Fig. 1, 3, 6, S2, S3, S4)

Partial protein sequence alignment of murine CCPs. The protein sequences of murine CCP1, CCP2, CCP3, CCP4, CCP5 and CCP6 were aligned with Clustal X (Chenna et al., 2003) and formatted using BoxShade (www.ch.embnet.org/software/BOX_form.html). Two residues in the highly conserved zinc-binding domain (Wang et al., 2006) were mutated (histidine to serine, glutamate to glutamine) for the generation of enzymatically dead versions of CCP1, CCP4, CCP5 and CCP6. Only the conserved portions of the full alignment are represented. Protein sequences were translated from cDNA sequences either taken from the database or from our reconstructed sequences for CCP4 and CCP6 (deposited in public databases with the accession numbers FN42927 and FN427928 respectively).



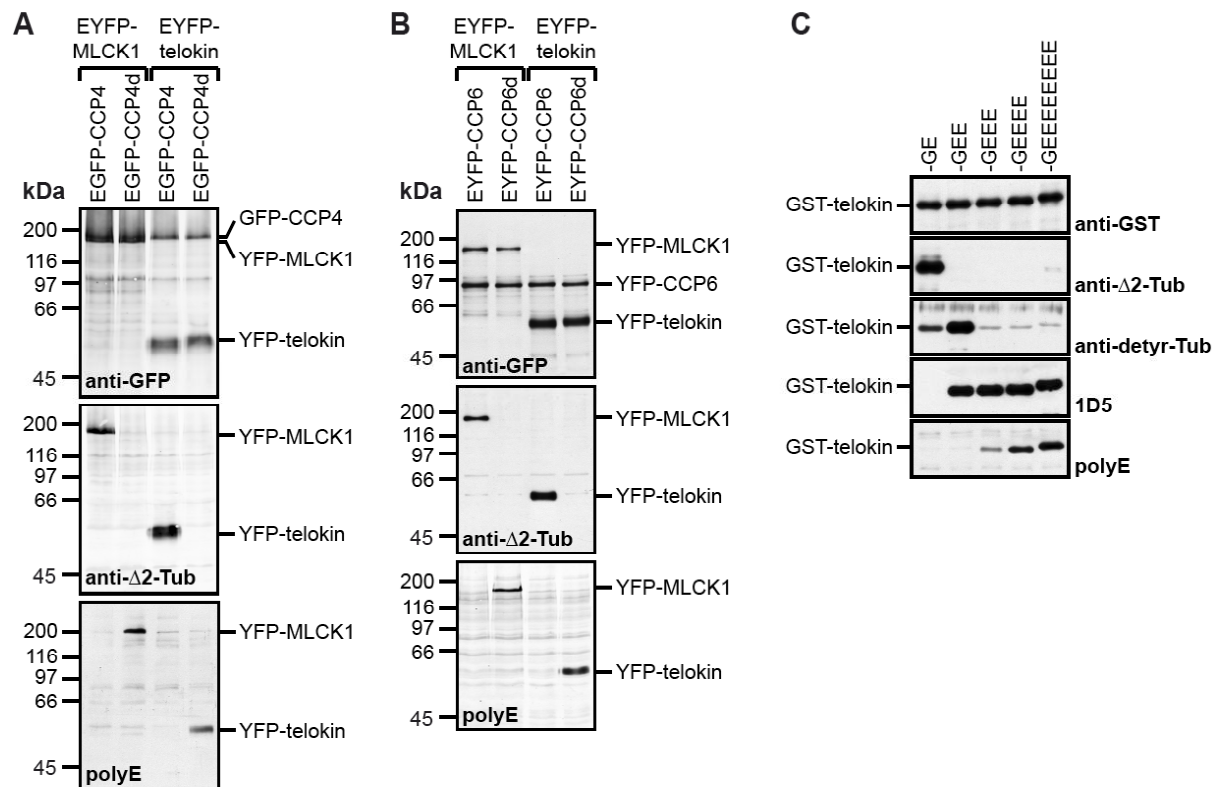
Supplementary Figure S2 Further characterization of CCP1 (related to Fig. 1)

(A) Immunofluorescence of mouse embryonic fibroblasts (MEFs) expressing EYFP-CCP1d (CCP1 carrying inactivating mutations as shown in Fig. S1). In contrast to active EYFP-CCP1 (Fig. 1B), EYFP-CCP1d does not result in ectopic appearance of anti-Δ2-tubulin labeling in the transfected cells. (B) Immunofluorescence of mouse hippocampal neurons expressing EYFP-CCP1d. In contrast to the expression of active EYFP-CCP1 (Fig. 1C), EYFP-CCP1d does not decrease the polyE labeling in the transfected cells. Scale bars in (A) and (B) are 20 μm. (C) CCP1 was expressed as a 6His-fusion protein in insect cells infected with baculovirus and purified on a Ni-column. Crude extracts from non-induced and induced insect cells, as well as the affinity-purified 6His-CCP1 were resolved on SDS page and stained with Coomassie brilliant blue. (D) *In vitro* assay with purified 6His-CCP1 and brain tubulin. Reactions containing 200 μg/ml of 6His-CCP1 and brain tubulin were incubated in the presence or absence of 10 mM phenanthroline for 6 h at 37°C. Brain tubulin is not detected with polyE antibody after incubation with 6His-CCP1, while GT335 reactivity remained. In the presence of the inhibitor phenanthroline, tubulin remains in the polyE-reactive form and is also detected with GT335. Total tubulin levels were adjusted with 12G10. This demonstrates that purified, recombinant CCP1 can remove long, but not short glutamate chains from purified brain tubulin.



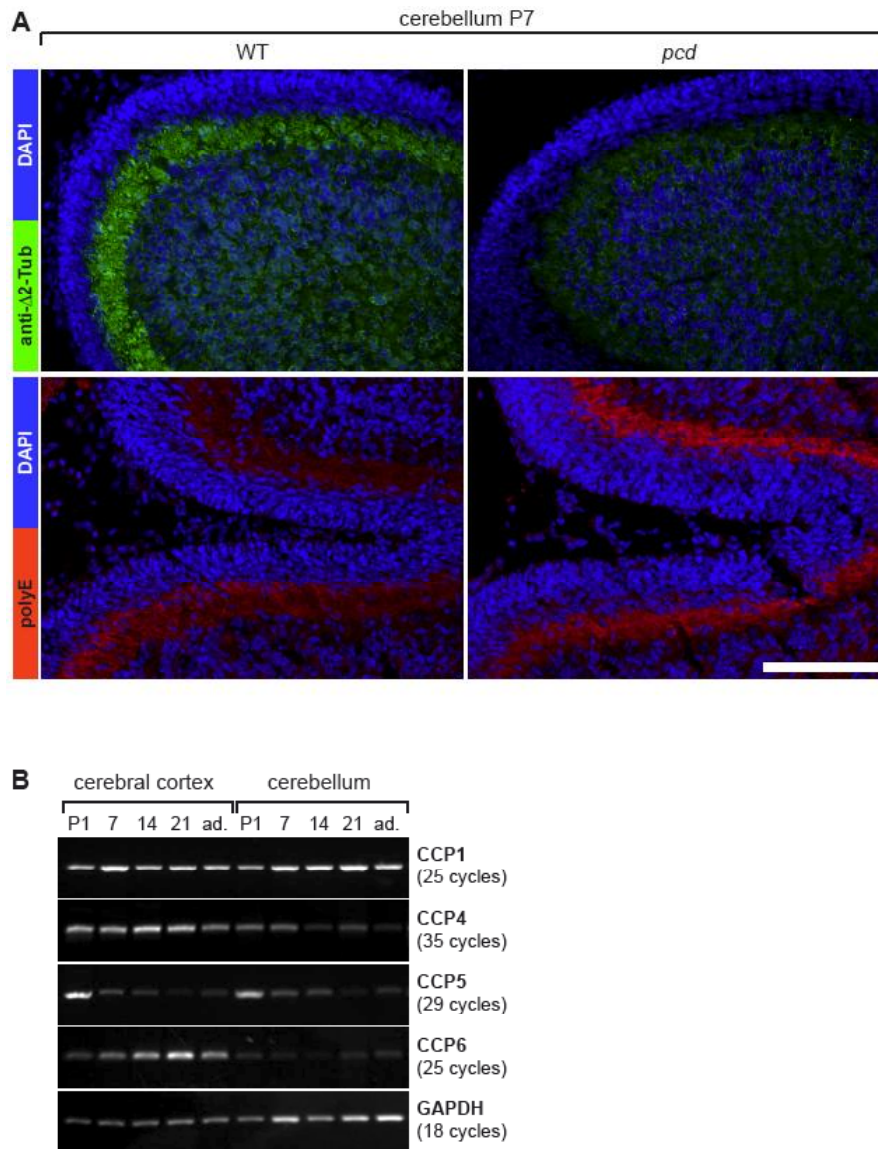
Supplementary Figure S3 Further characterization of CCP4 and CCP6 (related to Fig. 3)

(A) Immunofluorescence of mouse embryonic fibroblasts (MEFs) expressing EGFP-CCP4d or EGFP-CCP6d (CCP4 or CCP6 carrying inactivating mutations as shown in Fig. S1). In contrast to active EGFP-CCP4 and EGFP-CCP6 (Fig. 3A), both dead versions failed to induce anti- $\Delta 2$ -tubulin labeling in the transfected cells. Scale bar is 20 μ m. (B) Immunoblot of protein extracts from HEK293 cells expressing active (EGFP-CCP4) or inactive (EGFP-CCP4d) CCP4. In case of CCP4, the cells were grown in the presence of 5 μ M paclitaxel in order to increase the amount of detyrosinated tubulin in the cells (Gundersen et al., 1987). The paclitaxel treatment was required to detect $\Delta 2$ -tubulin generating activity of this enzyme. (C) Immunoblot of protein extracts from HEK293 cells expressing active (EYFP-CCP6) or inactive (EYFP-CCP6d) CCP6. (B, C) In both experiments, active, but not inactive CCP4 or CCP6 generated $\Delta 2$ -tubulin.



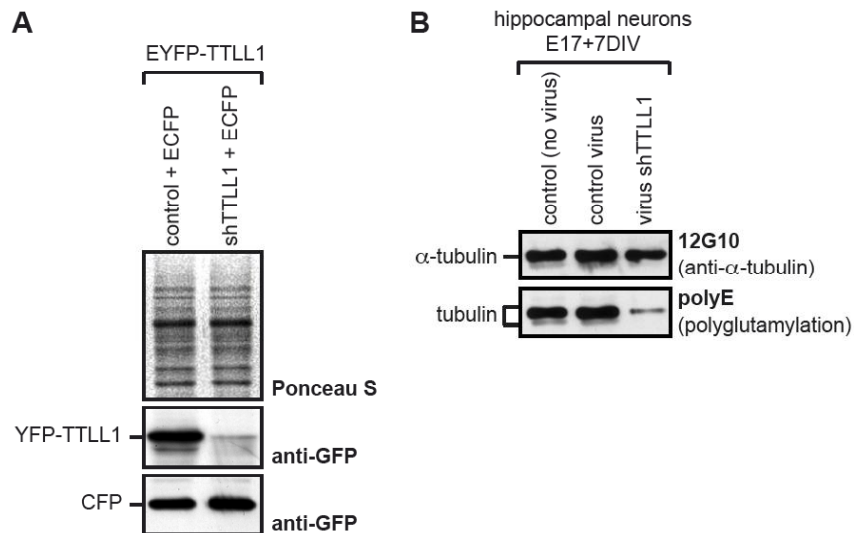
Supplementary Figure S4 Deglutamylation of MLCK1 and telokin (related to Fig. 2, 3)

(A, B) Immunoblots of protein extracts prepared from HEK293 cells co-expressing either (A) EGFP-CCP4 or (B) EYFP-CCP6 (or their respective inactive versions) together with either EYFP-MLCK1 or EYFP-telokin. The anti- Δ 2-tubulin antibodies label MLCK1 and telokin only when they were co-expressed with active CCP4 or CCP6, whereas polyE antibodies label MLCK1 and telokin co-expressed with inactive CCP4 or CCP6. (C) Antibody epitopes were mapped using artificial versions of telokin. Immunoblot of protein extracts prepared from *E. coli* strains expressing GST-telokin versions with different number of glutamic acids at their C-terminal tail. The tail regions are presented starting at glycine 151. Anti Δ 2-tubulin antibodies recognize exclusively telokin ending with a single glutamic acid. The anti detyr-tubulin antibodies strongly label telokin ending with two glutamates but also weakly recognize the other telokins. 1D5 antibodies recognize all telokins that carry two or more glutamates at their C-terminus. PolyE antibodies label telokins ending with three or more glutamates.



Supplementary Figure S5 Immunohistochemical and PCR analysis of *pcd* mice (related to Fig. 4)

(A) Immunohistochemistry of thin cerebellar sections from 7 d-old WT and *pcd* mice. Scale bar is 100 μ m. (B) Expression levels of CCP1, CCP4, CCP5 and CCP6 in cerebral cortex and cerebellum. RT-PCR was performed using cDNA from cerebral cortex or cerebellum of WT mice at different postnatal days. cDNA levels were normalized to the housekeeping gene glyceraldehyde 3-phosphate dehydrogenase (GAPDH). Compared to CCP1 and CCP6, CCP4 has a very low expression level considering that 35 instead of 25 PCR cycles are necessary for the amplification of a detectable PCR product. CCP1 is highly expressed throughout all stages of development in the two brain regions. In contrast, CCP6 is weakly expressed in cerebellum at all developmental stages, whereas its expression progressively increases during the development of the cortex. Expression levels of CCP5 decrease during development in both brain regions.



Supplementary Figure S6 Test of anti-TTLL1 shRNA efficiency (related to Fig. 5)

(A) Vectors expressing either shTTLL1 (H1-promotor) and ECFP (CMV promotor) or just ECFP were co-transfected together with an expression vector for EYFP-TTLL1 into HeLa cells. 20 h after transfection, cells were analyzed in immunoblot. Equal loading was controlled by staining the transfer membrane with PonceauS prior to immunoblotting. Expression of shTTLL1 completely suppresses the overexpression of EYFP-TTLL1, while in the control, EYFP-TTLL1 is strongly expressed. **(B)** One day old cultures of hippocampal neurons have been infected with control and shTTLL1 lentiviruses. Six days after infection, cells were lysed in SDS sample buffer and subjected to immunoblot analysis. In cells transfected with the control virus, polyE labeling is similar to the non-infected samples. Infection of hippocampal neurons with shTTLL1 virus strongly reduced tubulin polyglutamylation (polyE) levels.

Supplementary Table S1 (related to Fig. 2)

Summary of proteins identified in the anti- $\Delta 2$ -tubulin reactive 130 kDa protein band from stomach. The detailed mass spectrometry data are shown in Table S2. Note that only Myosin light chain kinase (N°4) has a C-terminal tail that can be processed by deglutamylation. See also Table S2

N°	Accession N°	Name	MW (kDa)	carboxy-terminal tail of identified protein	Total score	Coverage
1	Q9Z1Q9 SYV_MOUSE	Valyl-tRNA synthetase	140.2	-EAIALFQKML	37.83	25.1%
2	P16546 SPTA2_MOUSE	Spectrin alpha chain, brain	284.6	-VEFTRSLFVN	23.57	7.6%
3	O70133 DHX9_MOUSE	ATP-dependent RNA helicase A	149.5	-GRGGGGGGGY	17.67	11.0%
4	Q6PDN3 MYLK_MOUSE	Myosin light chain kinase, smooth muscle	212.9	-GEEEEEEEE	17.06	7.5%
5	Q6P5E4 UGGG1_MOUSE	UDP-glucose: glycoprotein glucosyltransferase 1 precursor	176.4	-QEGSQKHEEL	9.96	9.6%
6	Q8BTM8 FLNA_MOUSE	Filamin-A	281.2	-PGSPYRIMVP	8.82	4.7%
7	P09803 CADH1_MOUSE	Epithelial cadherin precursor	98.3	-ADMYGGGEDD	5.52	8.4%
8	Q8R2Y2 MUC18_MOUSE	Cell surface glycoprotein MUC18 precursor	71.5	-QGEKYIDLRLH	4.55	12.8%

Supplementary Table S2 (related to Fig. 2 and Table S1)

Complete mass spectrometry data on the analysis of the anti- $\Delta 2$ -tubulin reactive 130 kDa protein band from stomach. See *Excel file Rogowski_TableS2*

Supplementary Table S3 (related to Fig. 2)

Summary of proteins identified in the anti- $\Delta 2$ -tubulin reactive 20 kDa protein band from stomach. The detailed mass spectrometry data are shown in Table S4. Note that only Myosin light chain kinase has a C-terminal tail that can be processed by deglutamylation. *Although full-length MLCK was annotated, all reliable peptide hits correspond to the sequence of telokin. The sequence coverage of telokin is 30.2%. See also Table S4

N°	Accession N°	Name	MW (kDa)	carboxy-terminal tail of identified protein	Total score	Coverage
1	P63158 HMGB1_MOUSE	High mobility group protein B1	24.9	-EDEEEDDDDE	27.77	50.7%
2	P62827 RAN_MOUSE	GTP-binding nuclear protein Ran	24.4	-TALPDEDDDL	18.11	37.0%
3	P19157 GSTP1_MOUSE	Glutathione S-transferase P1	23.6	-NRPINGNGKQ	18.00	49.0%
4	Q9JM14 NT5C_MOUSE	5'(3')-deoxyribonucleotidase, cytosolic type	23.1	-GIIESKRASL	16.70	32.0%
5	P13745 GSTA1_MOUSE	Glutathione S-transferase A1	48.7	-QEARKAFKIQ	16.64	33.6%
6	Q99PT1 GDIR1_MOUSE	Rho GDP-dissociation inhibitor 1	23.4	-NLTIKKEWKD	16.02	38.2%
7	P14602 HSPB1_MOUSE	Heat shock protein beta-1	23.0	-AGKSEQSGAK	14.76	43.1%
8	Q9R1P3 PSB2_MOUSE	Proteasome subunit beta type-2	22.9	-ENIAFPKRDS	14.05	39.8%

9	P35700 PRDX1_MOUSE	Peroxiredoxin-1	22.2	-KSKEYFSKQK	14.00	38.2%
10	Q8VCR7 ABHEB_MOUSE	Abhydrolase domain- containing protein 14B	22.4	-GLLDFLQGLA	12.08	52.9%
11	P24472 GSTA4_MOUSE	Glutathione S-transferase A4	25.6	-VEVVRTVLKF	15.71	36.0%
12	Q9WVL0 MAAI_MOUSE	Maleylacetoacetate isomerase	24.3	-QPDTPAELRT	11.66	37.0%
13	P68033 ACTC_MOUSE	Actin, alpha cardiac muscle 1	42.0	-GPSIVHRKCF	11.40	23.3%
14	Q60631 GRB2_MOUSE	Growth factor receptor- bound protein 2	25.2	-NYVTPVNRNV	11.30	26.7%
15	P08249 MDHM_MOUSE	Malate dehydrogenase, mitochondrial	35.6	-KGEDFVKNMK	8.98	20.4%
16	P70195 PSB7_MOUSE	Proteasome subunit beta type-7	29.9	-EETVQTMDS	8.22	9.7%
17	P61087 UBE2K_MOUSE	Ubiquitin-conjugating enzyme E2	22.4	-ETATELLLSN	8.15	31.5%
18	Q6PDN3 MYLK_MOUSE	Myosin light chain kinase, smooth muscle*	212.9	-GEEEEEEEE	8.14	4.4%
19	Q04447 KCRB_MOUSE	Creatine kinase B-type	42.7	-AIDDLMPAQK	8.02	15.2%
20	P16858 G3P_MOUSE	Glyceraldehyde-3- phosphate dehydrogenase	35.8	-DLMAYMASKE	8.00	17.4%
21	Q9EPB4 ASC_MOUSE	Apoptosis-associated speck- like protein containing a CARD	21.4	-PYLVMDLEQS	8.00	19.7
22	O88587 COMT_MOUSE	Catechol O-methyltransfe- rase	29.5	-QPGSSPVKS	8.00	17.4%
23	P16110 LEG3_MOUSE	Galectin-3	27.5	-TLTSANHAMI	7.40	17.0%
24	Q9ET54 PALLD_MOUSE	Palladin	152.1	-NSGLVESEDL	7.00	5.0%
25	Q9CWF2 TBB2B_MOUSE	Tubulin beta-2B	50.0	-FEEEEGEDEA	6.42	9.7%

Supplementary Table S4 (related to Fig. 2 and Table S3)

Complete mass spectrometry data on the analysis of the anti- $\Delta 2$ -tubulin reactive 20 kDa protein band from stomach. *See Excel file Rogowski_TableS4*. Note that for hit N°18, reliable peptide hits (red) exclusively cover the telokin sequence.

Detailed experimental procedures

Cloning and mutagenesis

DNA sequences have been retrieved from the NCBI database (www.ncbi.nlm.nih.gov). The following sequences have been cloned from mouse cDNA and inserted into EYFP or EGFP tagged vectors: CCP1 (GI: 114158694), CCP2 (GI: 160420288), CCP3 (GI: 120300908), CCP5 (GI: 114150572), MLCK1 (the 130 kDa isoform of MLCK1; GI: 92122707) and telokin (GI: 11321439). CCP1 was also cloned into the pFastBac-HTb vector (Invitrogen). Sequences for CCP4 and CCP6 were reconstructed from genomic DNA, expressed sequence tags (ESTs) or cDNA sequences after BLAST homology search. EST and cDNA databases were screened by BLAST with mouse CCP4 (NM_172902) and CCP6 (NM_001048189) cDNA sequences to find novel sequences with new alternatively spliced exons. For CCP4, we found predicted cDNAs from horse (XM_001499739) and zebrafish EST (BI877247) containing additional 5' coding sequences. We also found a rat EST (AW534024/ DQ867033) containing a sequence encoding an alternative C-terminus terminated by a stop codon. For CCP6, we found the mouse ESTs CF724114/CO044549 and AV205871, the rat EST FM128597 and the human cDNA AK294394, all containing a novel CCP6 3' exon with a stop codon. Using these ESTs and cDNA sequences and comparing them to the exon analysis described in Kalinina et al., 2007, we identified 9 additional CCP4 exons (7 to extend the N-terminus and 2 to extend the C-terminus) and one additional CCP6 exon (for an alternative C-terminus). These novel isoforms of CCP4 and CCP6 were amplified from mouse brain cDNA, sequenced and used in the present study. The sequences have been deposited in public databases (accession numbers: CCP4: FN429927; CCP6: FN427928). In order to clone artificial telokin-like proteins that differ in their C-terminal sequences from wild type telokin, the MLCK1 cDNA was amplified with primers that contained the required sequence alterations (Fig. 2B-E; S4C). The PCR products were cloned into EGFP-, EYFP- or GST-tagged expression vectors and verified by sequencing.

Two point mutations were introduced into CCPs to generate enzymatically dead versions of the proteins (Fig. S1). We used a PCR-based quick-change method. The expression plasmids containing the cDNAs of the genes of interest were amplified with two mutagenic primers and Pfu polymerase (Promega). Template DNA was removed by digesting with Dpn I (NEB) for 4 h at 37°C; the DNA was then transformed into *E. coli* cells and single clones were isolated. The presence of the mutations was verified by DNA sequencing.

Mouse breeding and characterization

Mouse experiments were performed in accordance with institutional and national regulations, and have been approved by the local ethics committee. *Pcd* mice (BALB/cByJ-*Agtpbp1*^{*pcd-3J*}-J) were obtained from The Jackson Laboratories (www.jax.org). Mice strains were kept in the heterozygote state. For genotyping, genomic DNA was extracted from mouse-tails using the REExtract-N-Amp tissue PCR kit (Sigma), and three PCR reactions with specific primer pairs were performed.

For tissue preparation or cell culture, mice were sacrificed and organs were quickly dissected. Tissue extracts were prepared after snap freezing of the organs and grinding of the frozen material to a homogeneous powder. For immunoblot analysis, the powder was directly resuspended in Laemmli buffer, boiled for 5 min, sonicated and loaded onto SDS-PAGE.

For immunohistochemistry, mice were deeply anesthetized with pentobarbital (100-150 mg/kg, i.p.) and perfused transcardially with PBS, followed by 4% paraformaldehyde. The brains were removed, post-fixed in the same fixative overnight at 4°C, cryoprotected in 30% sucrose for 36 h at 4°C and embedded in tissue-freezing medium. 25 µm-thick coronal free-floating sections were collected for immunofluorescence.

For analysis of gene expression, total RNA was prepared from different mouse organs with TRIZOL[®] reagent (Invitrogen) according to the manufacturer's protocol. Total RNA content was determined at 260 nm and 5 µg of RNA were used for the synthesis of cDNA with the first strand cDNA synthesis kit (GE healthcare) following the manufacturer's protocol. PCR reactions were performed with Go-taq (Promega) in 25 µl using 2.5% of the total cDNA synthesis per PCR reaction. Primer pairs were chosen for the generation of approximately 1 kbp products. The size of the PCR-products was verified; a band of the predicted size was present in each reaction.

Lentivirus design and injection

TTLL1-specific shRNA was designed using standard algorithms and targets the GGACCTGATGGTGAAGAAC sequence of TTLL1. Hairpins were cloned into an shRNA expression vectors, which in parallel expresses ECFP from a separate promotor. To test shRNA efficiency, the constructs were co-transfected together with an EYFP-TTLL1 expressing plasmid (Janke et al., 2005), and the expression levels of EYFP-TTLL1 were analyzed by immunoblot.

The shRNA cassette was released from the expression plasmid and cloned into a lentivirus vector that co-expresses GFP from a separate promotor (Dittgen et al., 2004). Lentivirus vectors and expression plasmids for the proteins Gag, Pol and VSV-G were co-transfected into Lenti-X[™] 293T cells (Clontech). 2 d after transfection, the cell-free culture medium was spun at 80,000 g for 2 h at 4°C. The pellet was resuspended in RPMI medium supplemented with 1% BSA. Virus titers were determined by transducing Jurkat cells and scoring the transduction efficiency (GFP expression) using FACS analysis.

Mouse P10 pups were placed in a body silicon mold and anesthetized with 5% isoflurane for induction and with 2.5% isoflurane in 60% air / 40% oxygen for maintenance. After incision of the skin overlying the skull, a small hole was pinched directly over the left hemisphere of the cerebellum. One µl of lentivirus (containing about 10⁶ infectious particles) was injected into the cerebellum at a rate of 0.15 µl/min using a cannula directly connected to a micro-pump. After completion of the injections, the skin was sutured. Pups were returned to mother after recovery from anesthesia, and kept under standard housing. Injected mice were analyzed 30 d after injection (P40) using behavioral tests or immunohistochemistry.

Behavioral tests

Since in a pilot experiment, *pcd* mice were unable to maintain on a rotarod treadmill apparatus dedicated to mice, we assayed sensorimotor coordination using a larger rotarod (Ø 6 cm) dedicated to rats. Assays were performed on animals at P40, 30 d after virus injections (n=4). Mice were trained on the rotating cylinders at a constant speed of 4 rpm until they remained on the rod for at least 15 s (a maximum of 10 trials were done). To determine the latency to fall from the rod, the mice were placed on the rotating cylinder at 4 rpm, and the rotation was accelerated every 8 s by 1 rpm. Each mouse was assayed in 6 successive trials, and the average of

the 6 obtained values for each mouse was used to calculate the median. Significance was tested using the Mann and Whitney, non-parametric *t* test.

Tubulin purification

Pig brain tubulin was purified by two polymerization / depolymerization cycles followed by a phospho-cellulose column as described before (Vallee, 1986). Glutamylated tubulin was purified from HeLa cells 24 h after transfection with either TTLL4 for the generation of short glutamate side chains, or TTLL6 for long chains. Cells were lysed in PBS containing 0.2% NP40 and protease inhibitors. The cell lysate was spun for 20 min at 50,000 *g* at 4°C. The supernatant was loaded onto a GT335-affinity column prepared as previously described (van Dijk et al., 2008) and bound proteins were eluted with PBS containing 0.7 M NaCl and concentrated and desalted on an Amicon ultrafiltration device (4 ml, cut-off 30,000; Millipore) to a concentration of 1 mg/ml.

In vitro characterization of CCP activities

HEK293 cells were transfected with plasmids for the expression of CCP1, CCP4, CCP5 or CCP6 fused to either EGFP or EYFP. After 24 h, cells were collected, washed with PBS and lysed in PBS with 0.2% NP40 and centrifuged for 20 min at 50,000 *g* at 4°C. The supernatant was supplemented with different types of tubulin (pig brain tubulin or differentially modified tubulin from HeLa cells) and incubated at 37°C for 6 h and then directly subjected to SDS-PAGE. The modification status of tubulin was analyzed by immunoblot.

Recombinant GST-telokin was expressed in *E. coli* for 3 h. The cells were collected and sonicated in PBS, and soluble proteins were obtained by 30 min centrifugation at 50,000 *g* and 4°C. The supernatant was either used directly (Fig. S4C), or for telokin purification. In this case, the supernatant was incubated for 1 h with Glutathione Sepharose (GE healthcare) at 4°C and unbound proteins were washed off with PBS. GST-telokin was then eluted with 50 mM reduced glutathione pH 8.0.

Recombinant 6His-CCP1 was expressed in insect cells using the Bac-to-Bac baculovirus expression system according to the manufacturers protocol (http://kirschner.med.harvard.edu/files/protocols/Invitrogen_bactobacexpression.pdf). Briefly, baculovirus carrying the 6His-CCP1 construct were used to infect Sf9 insect cells. At signs of late infection, the cells were collected and lysed in Tris buffer (50 mM tris, pH 8.0, 100 mM NaCl, 1 mM EDTA, 10 mM β-mercaptoethanol) containing 0.1% Triton X100, and spun at 50,000 *g*, for 30 min at 4°C. Chelating Sepharose Fast Flow (GE healthcare) was incubated for 5 min with 200 mM NiSO₄, and subsequently washed in Tris buffer. The Ni-Sepharose was then incubated with the supernatant of the insect cell extract for 1 h at 4°C. The Ni-Sepharose was washed in Tris buffer containing 1 M NaCl, and 6His-CCP1 was eluted with Tris buffer containing 200 mM imidazole. The buffer was exchanged to PBS and 6His-CCP1 was incubated with either brain tubulin or recombinant GST-telokin for 6 h at 37°C. The modification status of the proteins was analyzed by immunoblot. As control, we added 10 mM of the carboxypeptidase inhibitor phenanthroline to the reaction (Felber et al., 1962).

Immunoprecipitation

Stomach and uterus from wild type mice were washed with PBS, frozen and ground to powder under liquid nitrogen. The powder was resuspended in PBS and 0.2% NP40, containing protease inhibitors, and centrifuged at 90,000 *g* for 20 min at 4°C. The supernatant was incubated for 2 h with DYNAL[®] protein G

coupled magnetic beads (Invitrogen) coated with anti-MLCK1 antibody (Sigma). The beads were then washed three times with PBS containing 0.2% NP40 and the bound proteins were analyzed by immunoblot.

Mass spectrometry

To identify the 130 kDa and the 20 kDa substrates of CCP1, stomachs were taken from wild type mice, washed with PBS, frozen and ground to powder in liquid nitrogen. The powder was resuspended in PBS supplemented with 0.2% NP40 and protease inhibitors, and centrifuged at 90,000 *g* for 20 min at 4°C. The supernatant was loaded onto a DEAE-column pre-equilibrated with PBS. The column was subsequently washed with PBS and bound proteins were eluted with 300 mM NaCl in PBS, and concentrated 35 times by centrifugation in an Amicon ultra-filtration device (4 ml, cut-off 10,000; Millipore). Proteins were resolved by SDS-PAGE and detected in parallel with Coomassie-brilliant blue staining and immunoblot with the anti- Δ 2-tubulin antibody. Bands of about 130 kDa and 20kDa, which were reactive with the anti- Δ 2-tubulin antibody, were excised from the Coomassie-stained gel and subjected to in-gel digestion with trypsin (Promega) as previously described (Shevchenko et al., 2006).

Peptides were resolved on an Ultimate 3000 nano-LC System (Dionex) equipped with a PepMap 100 C18 column (3 μ m particles, 10 nm pore size, 75 μ m x 15 cm). For MALDI MS/MS analysis, column effluent was mixed in a 1/3 ratio with MALDI matrix (2 mg/ml α -cyano-4-hydroxycinnamic acid (LaserBio Labs) in 0.1% TFA, 70% acetonitrile) and spotted on an Opti-TOF 384 Well Insert 123 x 81 mm plate (Applied Biosystems, Foster City, CA). MALDI plates were analyzed using the 4800 Plus MALDI TOF/TOF Proteomics Analyzer mass spectrometer (Applied Biosystems) in positive reflector ion mode. Each MS spectrum is the result of 1500 averaged laser shots. In MS/MS mode, fragmentation of automatically selected precursors was performed at a collision energy of 2 keV, each MS/MS spectrum is the result of 3000 laser shots. Peptide and protein identification were performed by ProteinPilot™ Software V 2.0 (Applied Biosystems) using the Paragon algorithm (Shilov et al., 2007).

Protein electrophoresis and immunoblot

SDS-PAGE was performed using standard protocols, or in the case of mammalian α - and β -tubulin by a special protocol as in (Eddé et al., 1987). Proteins were transferred onto Nitrocellulose membranes (Whatman) and detected with antibodies. Membranes were incubated with rabbit polyE (anti-polyglutamylation; 1:1,000), anti-GFP (1:5,000; Torrey Pines Biolabs), anti-GST (1:2,000), anti-detyrosinated tubulin (1:1,000; Chemicon) or anti- Δ 2-tubulin (1:4,000; gift of L. Lafanechère), mouse anti-MLCK1 (1:2,000, Sigma), GT335 (anti-glutamylation, 1:1,000 (Wolff et al., 1992), 6-11B-1 (anti-acetylated tubulin, 1:2,000; Sigma) and 12G10 (anti- α -tubulin; 1:500), or rat anti-tyrosinated tubulin (YL1/2; 1:5,000, Chemicon) antibodies. Protein bands were visualized with HRP-labeled donkey anti-rabbit, anti-mouse or anti-rat IgG 1:10,000 (GE Healthcare) followed by detection with chemiluminescence (ECL western blot detection kit, GE Healthcare). Alternatively, DyLight™ conjugated anti-mouse or anti-rabbit antibodies at 1:10,000 (Thermo Scientific) were used for detection with the Odyssey® Infrared Imaging System (Li-Cor® Biosciences).

For the graphical representation of modification levels in Fig. 4, protein bands from immunoblots were quantified using ImageJ software. After subtraction of the background, relative detection levels for modification-

specific antibodies were determined by adjusting the values to total tubulin levels (12G10 antibody). To determine the increase or decrease of tubulin modifications in the *pcd* mice, as compared to WT animals, the ratios between WT and *pcd* samples were plotted as percentage into bar diagrams.

Immunohistochemistry

Floating coronal sections were permeabilized for 45 min in PBS containing 0.3% (v/v) Triton X100 and 5% (v/v) normal goat serum (NGS). Slides were washed and incubated overnight with either mouse anti-calbindin D-28K (1:4,000; Swant) and rabbit anti-GFP (1:500; Invitrogen), or with anti- $\Delta 2$ -tubulin (1:2,000) or polyE (1:12,000) antibodies in PBS containing 0.1% Tween 20 and 1% NGS. Secondary antibodies were anti-mouse or anti-rabbit antibodies conjugated with either Alexa 555 or Alexa 488 fluorophores (1:1,000; Molecular Probes). After 45 min of secondary antibody incubation, nuclei were stained using either DAPI or Hoechst 33258. Fluorescent images were obtained with a LSM 710 confocal microscope (Carl Zeiss MicroImaging).

Cell culture, immunofluorescence and microscopy

Cerebellar granule neuron cultures were prepared from 7 d old murine pups (C57Bl/6 J mice) as described (Miller and Johnson, 1996) with slight modifications. Freshly dissected cerebella were incubated for 10 min at 37°C with 0.25 mg/ml trypsin and cells were dissociated in HBSS without Ca^{2+} and Mg^{2+} in the presence of 0.5 mg/ml trypsin inhibitor and 0.1 mg/ml DNaseI by several steps of mechanical disruption with a flame-polished Pasteur pipette. The resulting cell suspension was filtered through a 40 μm cell strainer (BD Falcon) and centrifuged at 200 g for 10 min. Cells were gently resuspended in K25+S medium (Basal Medium Eagle [BME] supplemented with 10% fetal bovine serum, 2 mM L-glutamine, 10 mM HEPES, penicillin-streptomycin (100 IU/ml-100 $\mu\text{g}/\text{ml}$) and 20 mM KCl), counted and seeded at a density of 25×10^4 cells/cm² in culture dishes previously coated with 20 $\mu\text{g}/\text{ml}$ poly-D-lysine (Becton Dickinson Biosciences). Granule neurons were cultured for 6 d, and 10 μM cytosine β -D-arabinofuranoside was added to the culture medium 24 h after plating. At 6 d *in vitro*, granule neurons represented more than 98% of cultured cells.

Cortical neuron cultures were prepared from embryonic day 17.5 (E17.5) swiss mouse embryos as described previously (Lesuisse and Martin, 2002) with slight modifications. Freshly dissected cortices were digested in the presence of 0.25% trypsin for 15 min at 37°C and cells were dissociated by several steps of mechanical disruption with two flame-polished Pasteur pipettes of decreasing diameter. The resulting cell suspension was filtered through a 70 μm cell strainer (BD Falcon). Cells were diluted to 10^6 cell/ml with MEM medium (Invitrogen), supplemented with penicillin/streptomycin (Invitrogen), 0.6% (w/v) glucose (Sigma) and 5% (v/v) fetal bovine serum and seeded at a density of 10^3 cells/mm² in culture dishes previously coated with 20 $\mu\text{g}/\text{ml}$ poly-D-lysine (Becton Dickinson Biosciences). After 3-4 h, the medium was exchanged for Neurobasal medium (Invitrogen), supplemented with penicillin/streptomycin (Invitrogen), GlutaMAX-I, B27 supplement (Invitrogen) and 25 μM β -mercapto ethanol. Cells were cultured at 37°C in a humidified incubator with 5% CO_2 / 95% air. To prevent proliferation of remaining non-neuronal cells, 10 μM cytosine β -D-arabinofuranoside was added to the culture medium 3 d after plating.

Mouse embryonic fibroblasts (MEFs) were prepared from E13.5 embryos following standard procedures. MEFs, HeLa, U2OS or HEK293 cells were cultured on plastic dishes or glass coverslips under standard conditions. Expression plasmids were transfected using JetPEI (Polyplus transfectionTM) or Amaxa Biosystems.

Cells were fixed using a protocol for preservation of cytoskeletal structures (Bell and Safiejko-Mroczka, 1995), or with methanol at -20°C. Cells were then incubated with GT335 (1:3,000), polyE (1:1,500), anti- $\Delta 2$ -tubulin (1:6,000) or anti-tyrosinated tubulin (YL1/2; 1:6,000) antibodies for 1 h, followed by 30 min with anti-mouse, anti-rabbit or anti-rat antibodies conjugated with either Alexa 555 or Alexa 488, Cy3 or Cy5 fluorophores (1:1,000; Molecular Probes). DNA was visualized by DAPI (4',6-diamidino-2-phenylindole; 0.02 $\mu\text{g/ml}$) or Hoechst (1 $\mu\text{g/ml}$) staining. Coverslips were mounted with MOWIOL or Dako mounting medium. We used DMRA (Leica) or Axioskop 50 (Carl Zeiss MicroImaging) microscopes, and images were acquired using Metamorph (Universal Imaging Corp.) software.

Supplementary references

- Bell, P.B., Jr., and Safiejko-Mroczka, B. (1995). Improved methods for preserving macromolecular structures and visualizing them by fluorescence and scanning electron microscopy. *Scanning Microsc* 9, 843-857; discussion 858-860.
- Chenna, R., Sugawara, H., Koike, T., Lopez, R., Gibson, T.J., Higgins, D.G., and Thompson, J.D. (2003). Multiple sequence alignment with the Clustal series of programs. *Nucleic Acids Res* 31, 3497-3500.
- Dittgen, T., Nimmerjahn, A., Komai, S., Licznanski, P., Waters, J., Margrie, T.W., Helmchen, F., Denk, W., Brecht, M., and Osten, P. (2004). Lentivirus-based genetic manipulations of cortical neurons and their optical and electrophysiological monitoring in vivo. *Proc Natl Acad Sci U S A* 101, 18206-18211.
- Eddé, B., de Nechaud, B., Denoulet, P., and Gros, F. (1987). Control of isotubulin expression during neuronal differentiation of mouse neuroblastoma and teratocarcinoma cell lines. *Dev Biol* 123, 549-558.
- Felber, J.-P., Coombs, T.L., and Vallee, B.L. (1962). The mechanism of inhibition of carboxypeptidase A by 1,10-phenanthroline. *Biochemistry* 1, 231-238.
- Gundersen, G.G., Khawaja, S., and Bulinski, J.C. (1987). Postpolymerization detyrosination of alpha-tubulin: a mechanism for subcellular differentiation of microtubules. *J Cell Biol* 105, 251-264.
- Lesuisse, C., and Martin, L.J. (2002). Long-term culture of mouse cortical neurons as a model for neuronal development, aging, and death. *J Neurobiol* 51, 9-23.
- Miller, T.M., and Johnson, E.M., Jr. (1996). Metabolic and genetic analyses of apoptosis in potassium/serum-deprived rat cerebellar granule cells. *J Neurosci* 16, 7487-7495.
- Shevchenko, A., Tomas, H., Havlis, J., Olsen, J.V., and Mann, M. (2006). In-gel digestion for mass spectrometric characterization of proteins and proteomes. *Nature Protocols* 1, 2856-2860.
- Shilov, I.V., Seymour, S.L., Patel, A.A., Loboda, A., Tang, W.H., Keating, S.P., Hunter, C.L., Nuwaysir, L.M., and Schaeffer, D.A. (2007). The paragon algorithm, a next generation search engine that uses sequence temperature values and feature probabilities to identify peptides from tandem mass spectra. *Molecular & Cellular Proteomics* 6, 1638-1655.

Supplemental Figure S1

[Click here to download Supplemental Figure: Rogowski_FigS1.eps](#)

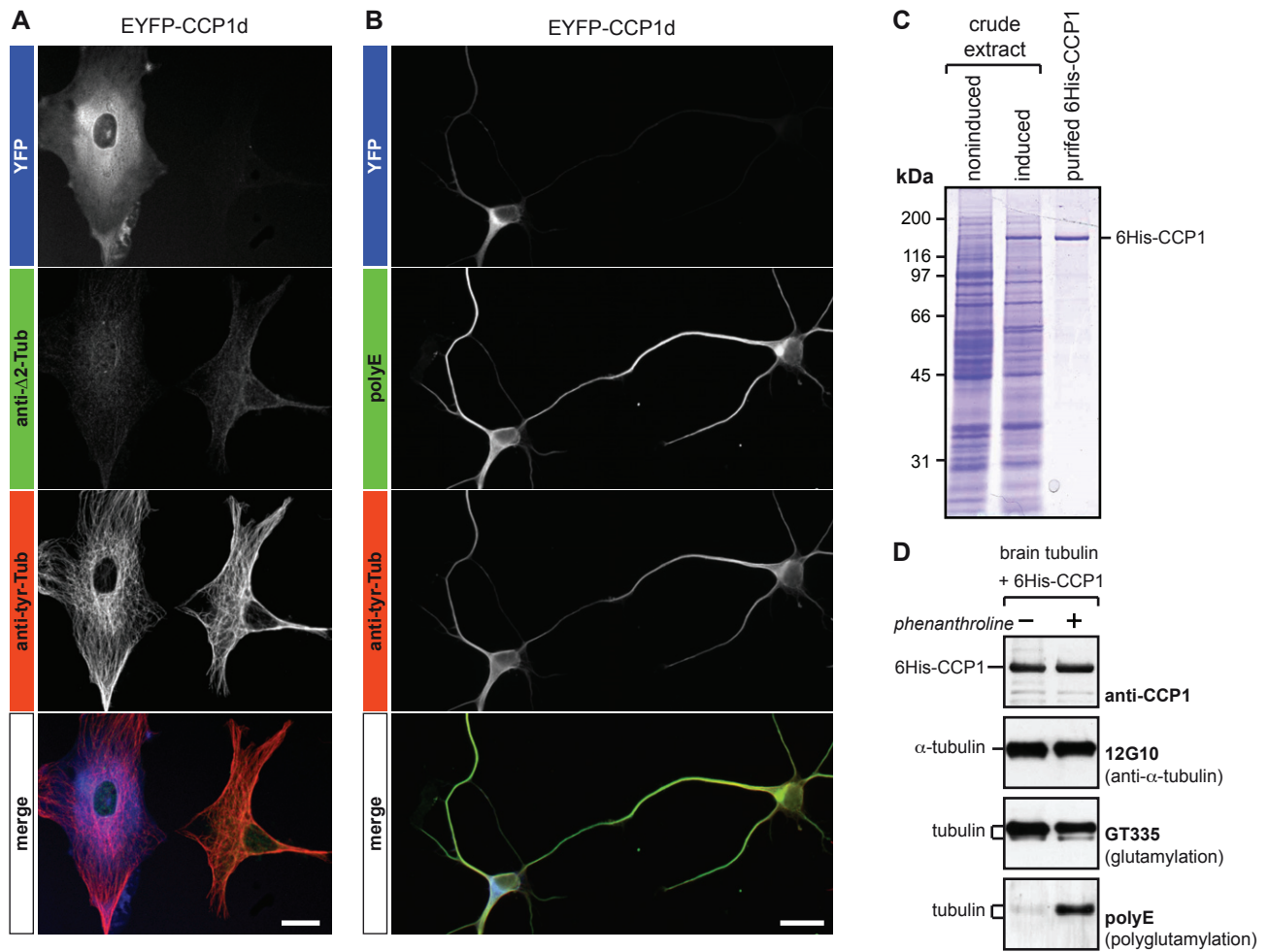
```
CCP1 631 SVPEYSEVYDPDFCHIPPFFKEPIERPYCVORTKTAQDERIHHQNDIIDRVVYLDNPTTYTTPPEGDTLTKNSKTFESGNLRKVIQIR
CCP2 178 PEIVGEEQTVVYQLDSPBAEGTYFTSSRIGGKRGTIKELAVTLOGP-----DDNTLFFESRFESGNLQKAVRVG
CCP3 123 PVYPNSKEDTVVYLAEDAYKEP-CFVYSRVGGVRTSKQPVDFNC-----DNLTLVFEARFESGNLQKVVKVA
CCP4 522 SAVGFKTMFPDLWCHCPFPAAQPMDRKLGVRIRIKILEDERRLLHPSDVINKVVFSLDEPRPLOGSISNCLMBHSKTFESGNLRKALQVR
CCP5 39 ATAPASG-----SAASP
CCP6 39 PPK-----GHLTFDACEFESGNLGRVQVS

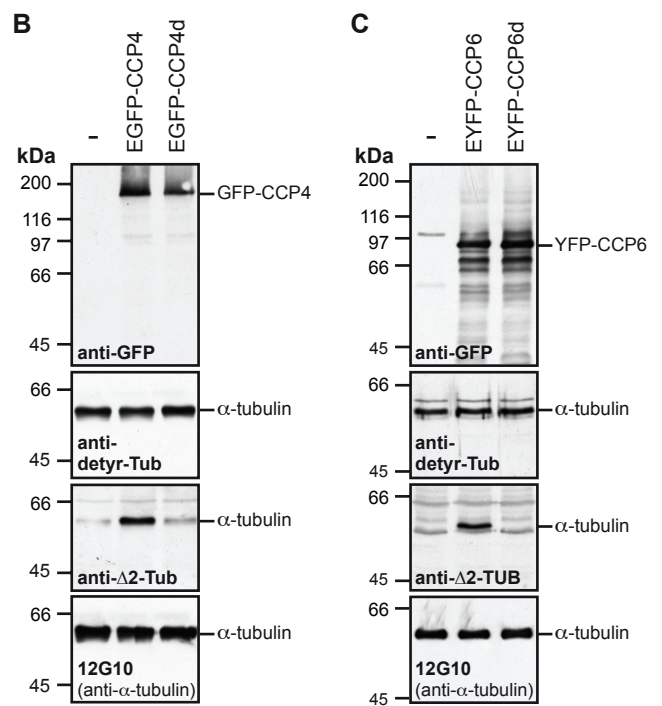
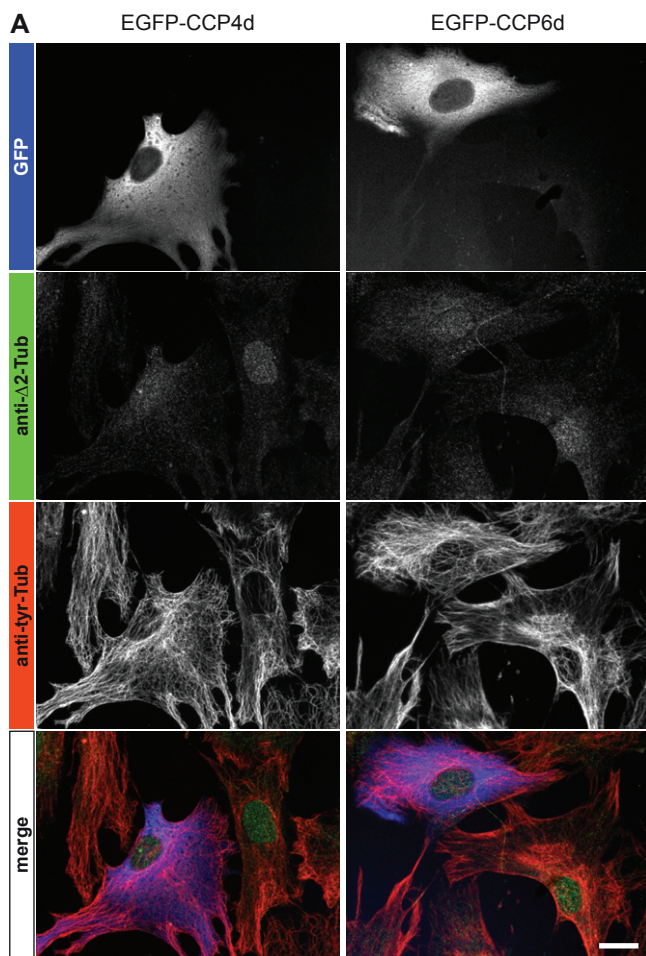
CCP1 721 KSEYDLEINSDINSNYH---QWFYEVSGMRPGVAYRFNINCEKSNQENVMGMOPLMYSVQEAENAREPWWIRMGDITCYKKNHFSRS
CCP2 248 IMEYELTLRFDLYDKHT---QWFYFRVQNTKDATYRFTIVNLLKPKSLYAVGMKPLMYSQDATIYNICWRREGRETKYKKNV---
CCP3 188 DHEYELTLVRPDLFNKHT---QWFYFOVNTQAEIVYRFTIVNFTKPAASLYNRGMKPLFYSEKEAKTHNICWORIQDQIKYKKNL---
CCP4 612 EPEYDLELVNADVNSOHO---QWFYFKVSGMRAAVPYHFNINCEKPNQENVMGMOPTLYSVKEALLGRFAWRIRGSDITCYKKNHYRON
CCP5 51 DVEFNWTRPDCAEETEYENGRSFWYFSVRGGTFCCLKIKINIMNMQSKLYSQGMAFVRT---LPSRPRWRIRERPTEEMT----
CCP6 63 DPEYDLELRPDCNCPFR---VWFNEITVENVRELORVIFNIVNFSKTKSLYRDGMAFMVKSS---TS-REKWRQLPPKKNVYYR----

CCP1 807 SVAAGCQKGSYHITFTVNFPHKO-DVCYFAYHYPTYSTLQMHLOKLES-----AHNPOQIVFRKDVLCETISGNICPLVTTITA
CCP2 331 ---DDGQOPLVCLTWTTFPHDQ-DTCYFAHFYPTYLDLOCYLLSVAN-----NP-TQSQCRRLRALCRSLAGNTVYLLTITN
CCP3 271 ---GQGRHFSLTWTTFPHSQ-DTCYFAHCYPPTYSNLOEYLSGINS-----DP-VRSKCRIRVLCHILARNMVYLLTITN
CCP4 698 AATMDCALGKRYHLEAVTFPHN-DACYLAFHYPTYSTLTHLETLER-----SIDHRETVFRHDVLCQILGGNCPCLVTTITA
CCP5 132 ---ETQVLEFVHREVEGRGATTEFAFCYFPYSYSDCDDLSQLQRFSENYSTHSSP-DSTVYHREILCYSDGLRVOLLTITS
CCP6 139 ---CPDHRKNVMSEAFCDRED-DIYQFAYCYPPTYLRFQHYLDSLOK-----KN-MDYFER-EOLGQSVQQRQLDLLTITS

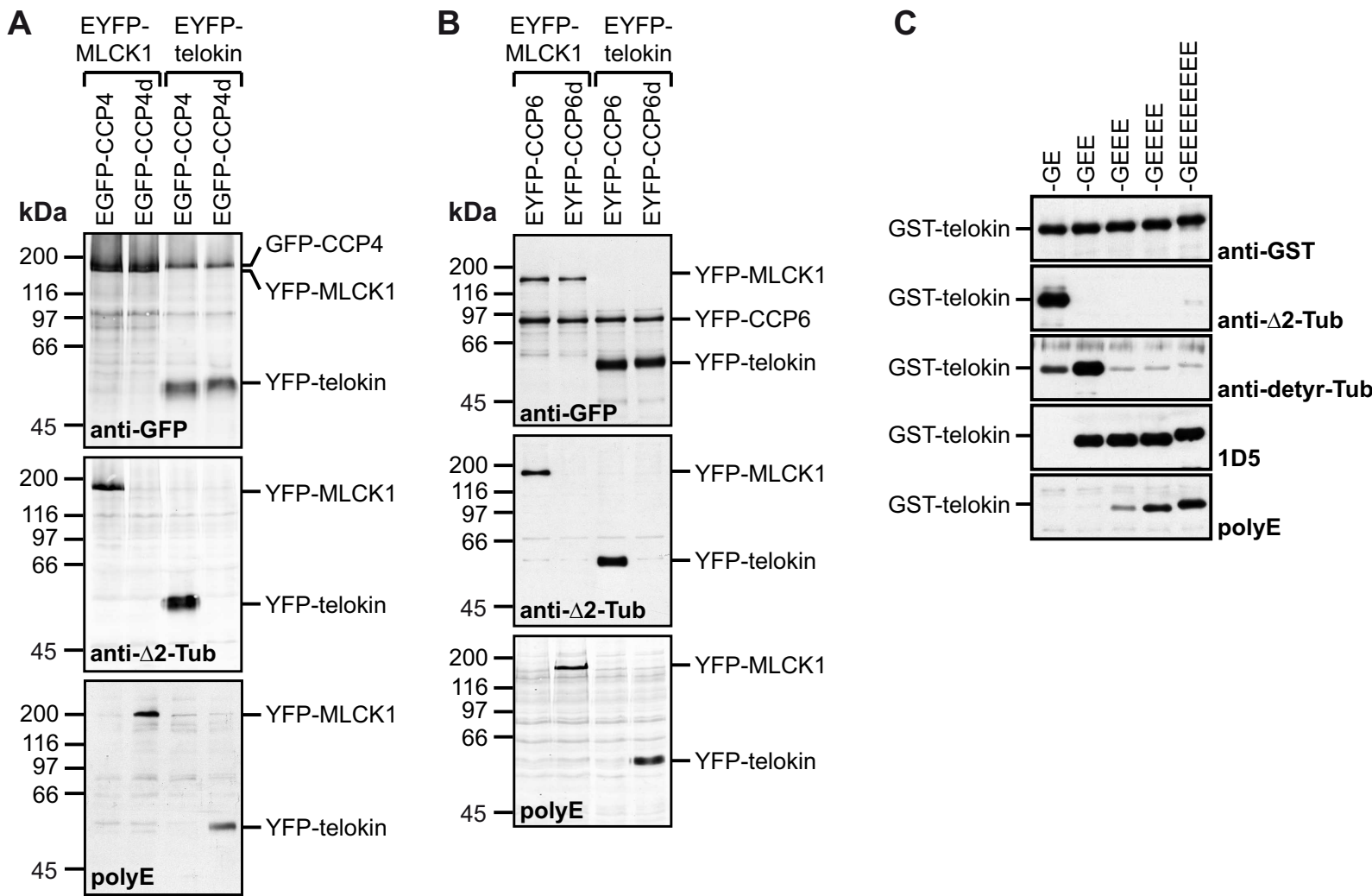
CCP1 887 MPESNY-----YEICQERTFPHYFLSARVHPGETNASWVMKGTLEYLMS-NSPTAQSLRESYIFKVIIPMLNPDGVINGNH
CCP2 405 PSRTP-----QEAAAANKAVLSARVHPGESNSSWIMNGFLDFLLS-NSPDAQLLRDFVFKVIIPMLNPDGVIVGNY
CCP3 345 PLKT-----SDSKRKAAILLVARVHPGETNSSWIMKGFLDYILG-DSSDARLLRDFIFKVIIPMLNPDGVIVGNY
CCP4 778 FPEENS-----TELEQFRCPYQVILVARVHPGESNASWVMKGTLEFLVS-SDEVAKLLRENFVFKVIIPMLNPDGVINGNH
CCP5 213 CHGLRDDREPRLEQLFPDLGTPPFRETKRIRIFLSRVHPGETPSSFVFNGLDFLLRPDDRAQTLRRLFVFKVIIPMLNPDGVIVGNY
CCP6 211 PENLR-----EGSEAKVIFITGRVHPGETPSSFVCOGTLDFLVS-CHPTARVLRHLVFKVIIPMLNPDGVIVGNY

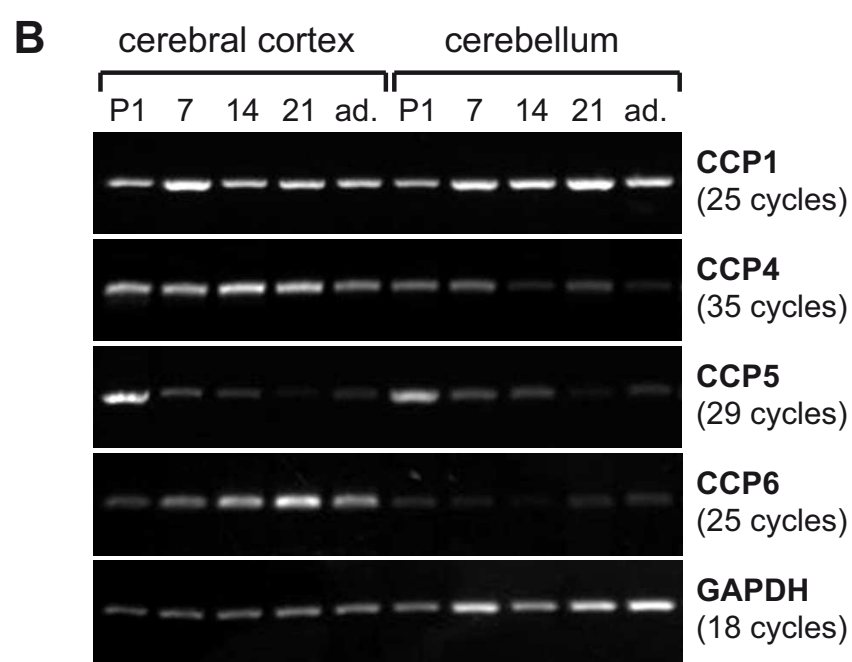
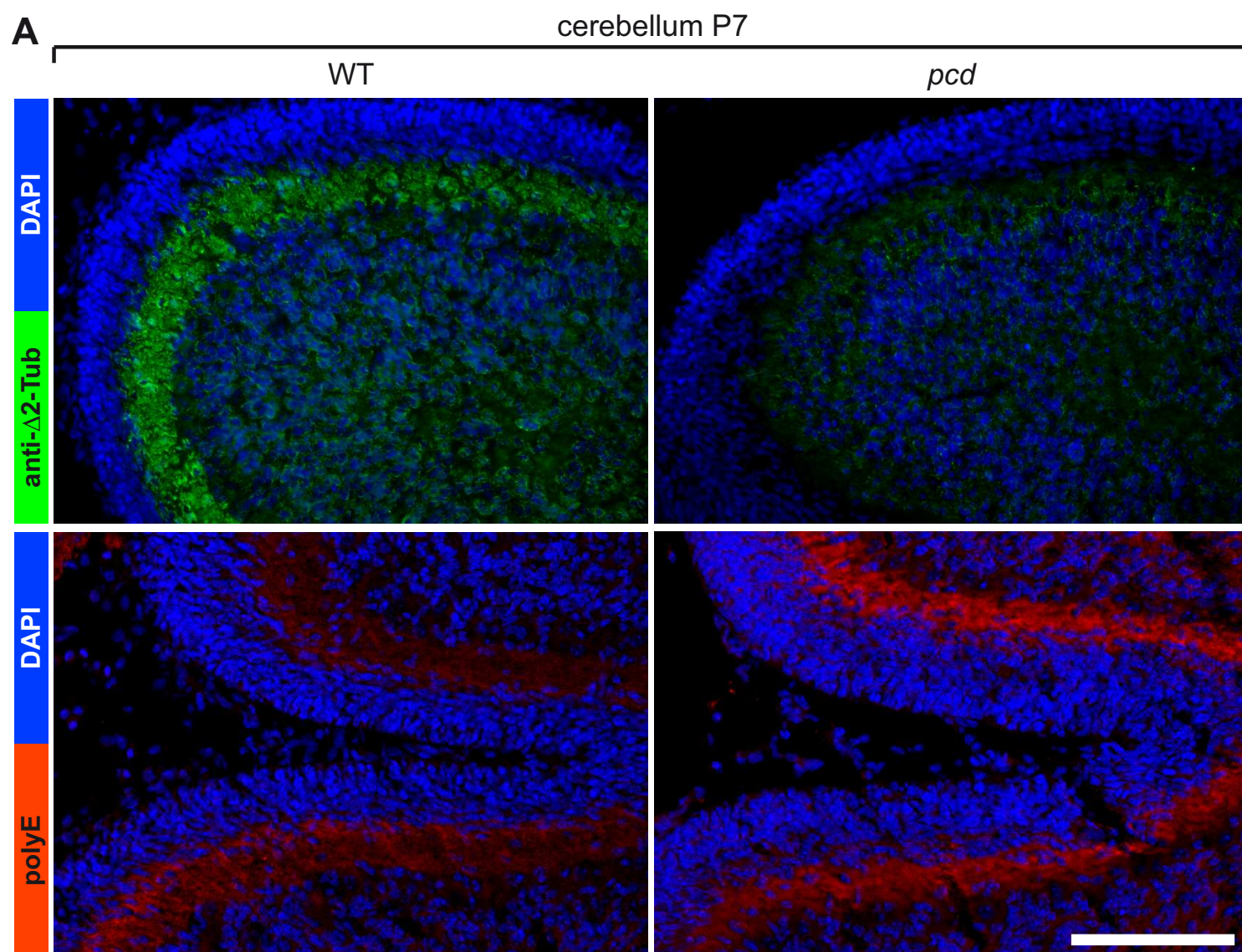
CCP1 962 RCSLSCEDLNROQSPNPELHPTTYHAKGLLOYLAA-V-----
CCP2 475 RCSLACRDLNRHKTVLKDSFPCIIWYTKNMIKRILLE-----
CCP3 413 RCSLACRDLNRNYTSLKESFPSVWYTRNMINRIME-----
CCP4 853 RCSLRCEDLNROQLSQAHLQPTTYHAKGLLHYLSS-T-----
CCP5 303 RTDSRCVNLNROQLKPDVLLHPALYCAKAVLLHHVHSRLNAKSPNTQOQPTLHLPPEAPLSDLEKANNLHNEAHLGQSPDGENPATWPET
CCP6 280 RCSLMCFDLNRHLDPSWAHPETHGVKQLLIKLYNDP-----
```





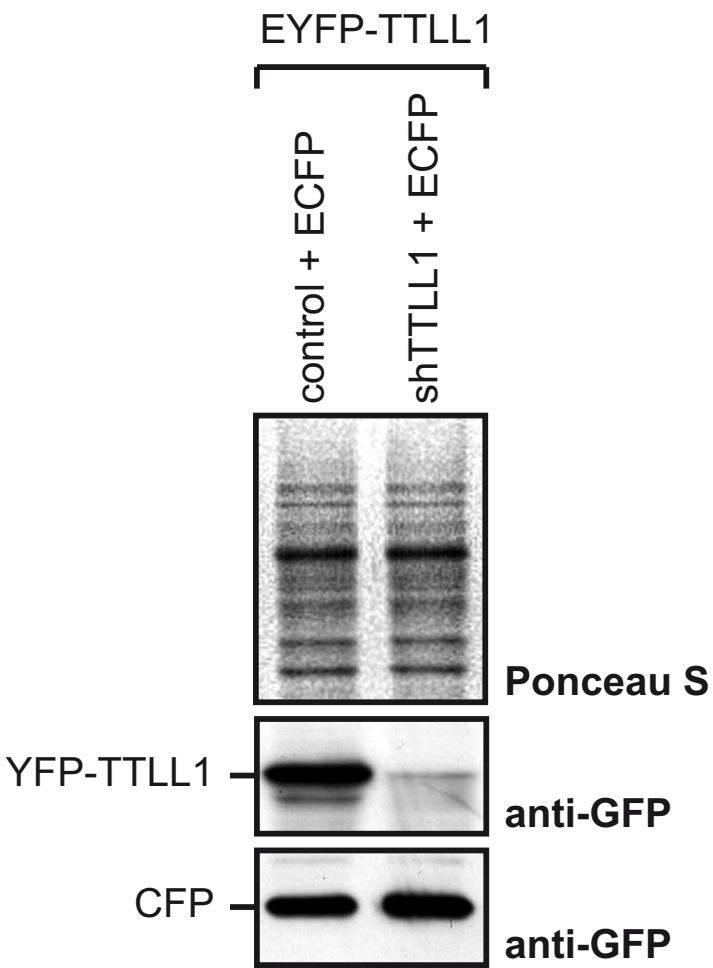
Rogowski et al., supplementary Figure S4



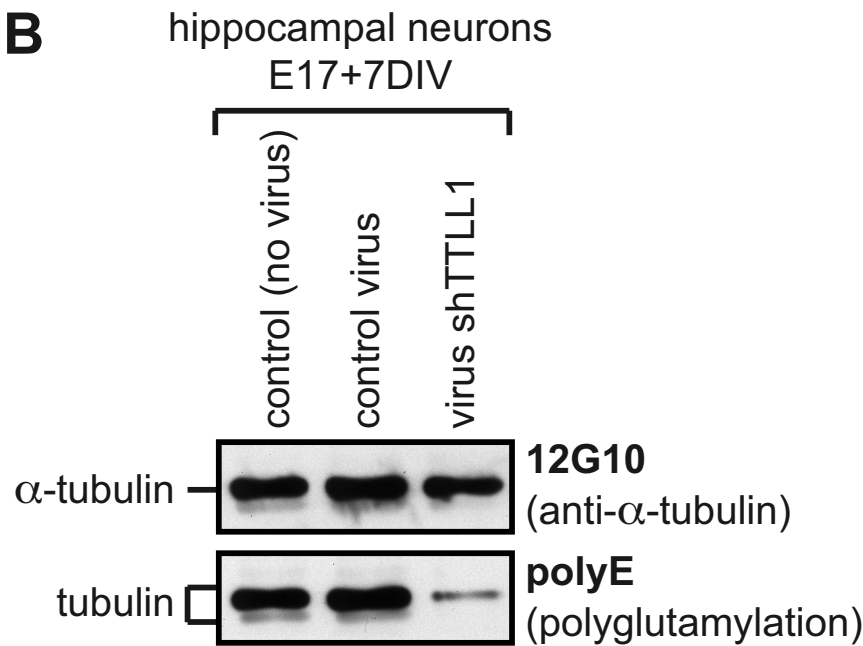


Rogowski et al., Figure S6

A



B



Polyglutamylation is a reversible posttranslational protein modification for which only forward enzymes are known. In their article, Rogowski et al. present the discovery of several protein deglutamylases as members of the cytosolic carboxypeptidase family and describe the enzymatic mechanism of protein deglutamylation. In addition, they show that some of these enzymes also remove gene-encoded glutamates from the carboxy-terminus of proteins including an important regulator of myosin function, myosin light chain kinase. Finally, by analyzing the *purkinje cell degeneration (pcd)* mice that lack activity of one of these newly discovered deglutamylases, the authors show that hyperglutamylation is directly linked to neurodegeneration.

Cell Conflict of Interest Form

Cell Press, 600 Technology Square, 5th floor, Cambridge, MA 02139

Please complete this form electronically and upload the file with your final submission.

Cell requires all authors to disclose any financial interest that might be construed to influence the results or interpretation of their manuscript.

As a guideline, any affiliation associated with a payment or financial benefit exceeding \$10,000 p.a. or 5% ownership of a company or research funding by a company with related interests would constitute a financial interest that must be declared. This policy applies to all submitted research manuscripts and review material.

Examples of statement language include: AUTHOR is an employee and shareholder of COMPANY; AUTHOR is a founder of COMPANY and a member of its scientific advisory board. This work was supported in part by a grant from COMPANY.

Please disclose any such interest below on behalf of all authors of this manuscript.

Please check one of the following:

- None of the authors of this manuscript have a financial interest related to this work.
- Please print the following Disclosure Statement in the Acknowledgments section:

Please provide the following information:

- Please check this box to indicate that you have asked every author of this work to declare any conflicts of interest. Your answers on this form are on behalf of every author of this work.

Manuscript #: CELL-D-10-00175

Article Title: A family of protein deglutamylating enzymes associated with neurodegeneration

Author List: Krzysztof Rogowski, Juliette van Dijk, Maria M. Magiera, Christophe Bosc, Jean-Christophe Deloulme, Anouk Bosson, Leticia Peris, Nicholas D. Gold, Benjamin Lacroix, Montserrat Bosch Grau, Nicole Bec, Christian Larroque, Solange Desagher, Max Holzer, Annie Andrieux, Marie-Jo Moutin, Carsten Janke

Your Name: Carsten Janke

Date: 20 September 2010